



Differential heavy quark pair production at small x

Federico Silvetti^{1,2,3,a} , Marco Bonvini^{2,b}

¹ Dipartimento di Fisica, Sapienza Università di Roma, Piazzale Aldo Moro 5, 00185 Rome, Italy

² INFN, Sezione di Roma 1, Piazzale Aldo Moro 5, 00185 Rome, Italy

³ Theoretical Physics Department, CERN, 1211 Geneva 23, Switzerland

Received: 23 November 2022 / Accepted: 12 February 2023
© The Author(s) 2023

Abstract We consider the production of a heavy quark pair in proton–proton collisions. For bottom and charm quarks, the final state invariant mass is typically much smaller than the collider energy (e.g. at the LHC), so that high-energy logarithms may spoil the perturbativity of the theoretical prediction at fixed order. The resummation of these logarithms to all orders is thus needed to obtain reliable predictions. In this work, we extend previous results on high-energy (or small- x) resummation to differential distributions in rapidity, transverse momentum and invariant mass, and implement them in the public code HELL.

Contents

1	Introduction
2	Multi-differential small- x resummation in HELL
2.1	Extension of k_t factorization to differential observables in pp collisions
2.2	Small- x resummation of differential distributions in the HELL language
2.3	All partonic channels
2.4	Matching to fixed order
3	Heavy-quark pair production
3.1	Results differential in the single heavy-quark
3.2	Results differential in the heavy-quark pair
4	Conclusions
Appendix A: The off-shell coefficient function	
A.1	Kinematics for the single quark
A.2	Kinematics for the pair
A.3	Matrix element
A.4	On-shell limit

Appendix B: Simplifications in the resummation formulae for pair kinematics
References

1 Introduction

In the era of LHC precision physics, considerable efforts are required to match theoretical prediction with experimental accuracy. Such an endeavour requires several different inputs, e.g. high-order predictions for partonic processes, high-quality parton distributions and all-order resummation of large logarithmic contributions.

In this work, we focus on the latter and specifically on the so-called high-energy logarithms of the form $\alpha_s^n \frac{1}{x} \log^k \frac{1}{x}$, $k < n$, where x is a dimensionless scaling variable that becomes small when the collider energy s is large. These perturbative terms arise beyond the leading order in both the partonic cross sections and the DGLAP splitting functions governing PDF evolution (in $\overline{\text{MS}}$ -like schemes). At the energy scales of many LHC processes, $x \ll 1$ and these logarithms spoil the perturbativity of the fixed-order results. This calls for an all-order resummation of these corrections.

The theoretical framework to perform this high-energy (or small- x) resummation has been established during the last 30 years starting with the resummation of splitting functions [1–16] by means of the Balitsky–Fadin–Kuraev–Lipatov (BFKL) equation [17–22] and arriving recently to PDF determination with resummed theory [23–25].

One of the key steps to achieve a consistent resummed prediction is the resummation of partonic cross sections, which can be carried out to leading logarithmic (LL) precision using the k_t factorization theorem [26–28]. Recently, the resummation technique for partonic cross sections has been reformulated and adapted for stable numerical implementation [29–31]. This led to the release of the High-Energy Large Logarithms (HELL) public code, which aims to provide a

^a e-mail: federico.silvetti@uniroma1.it (corresponding author)

^b e-mail: marco.bonvini@roma1.infn.it

systematic framework for implementing small- x resummation.

So far, only inclusive observables have been considered in HELL. The sensitivity of inclusive observables to resummation effects is, however, limited. Indeed, the small- x region at parton level is mixed with the medium- and high- x regions in the convolution that defines the hadron-level cross section, thereby smoothening out much of the impact of high-energy logarithms (see e.g. Ref. [31]). Differential distributions, instead, can be more directly sensitive to specific values of partonic x , thereby enhancing the effect of small- x resummation in some kinematic regions. Moreover differential distributions are of greater phenomenological interest, as they can be compared more directly with experimental measurements.

In this work we will focus on invariant mass, rapidity and transverse momentum distributions. The resummation of small- x logarithms in these differential cross sections was developed in Refs. [32–34], focussing on Higgs production via gluon fusion. Here, we revisit these results and extend them to the modern resummation formalism of Refs. [29–31], thereby allowing for a stable numerical implementation thus opening the door to phenomenological studies.

We apply our findings to heavy flavour pair production, and construct resummed predictions for distribution in invariant mass, rapidity and transverse momentum of either the heavy-quark pair or one of the heavy quarks. This process is particularly interesting due to the availability of measurements from the LHCb experiment for the production of charm and bottom quarks in the forward region, where one of the incoming partons is certainly at small x and thus the effect of resummation should be marked. In addition, these data reach values of x down to $x \sim 10^{-6}$, which is a region of proton momentum fractions so far unexplored, as the HERA data is limited to $x \gtrsim 3 \cdot 10^{-5}$ in the perturbative regime. Our results thus provide an important ingredient to refine the determination of PDFs at small- x , which serves both as a test of QCD in extreme regimes and as a tool to improve high-energy phenomenology. All our results are available through the new release of the HELL code.

The structure of this paper is the following. Section 2 is dedicated to presenting the formalism of k_t factorization in a proton collider and its use to construct small- x resummed results for differential distributions in the language of HELL. Then, Sect. 3 is dedicated to the application of resummation to differential heavy flavour production, parametrising the final state respectively as the entire quark-antiquark pair or as a single quark. We conclude in Sect. 4, and collect in the appendices various details on analytical expressions for heavy quark production and aspects of numerical implementation.

2 Multi-differential small- x resummation in HELL

The resummation of small- x logarithms in physical observables is based on k_t factorization [26–28, 35–37]. The basic observation is that the leading small- x logarithms arise, in a physical gauge, from k_t integration over gluon exchanges in the t channel. Therefore, in the small- x limit, the generic amplitude squared can be decomposed into contributions that are two-gluon irreducible (2GI) in the t channel and thus do not contain any logarithmic enhancement. Instead, the small- x logarithms are produced by the integration over the momenta of the gluons connecting these 2GI block. In this way the cross section of the process factorizes [26–28] into a process dependent 2GI coefficient, called off-shell coefficient function, and process independent “unintegrated” PDFs that contain the traditional collinear PDFs and the sum over all possible process independent 2GI kernels connected by off-shell gluons. By making explicit the dependence of unintegrated PDF on collinear PDFs and comparing the result with the standard collinear factorization, one finally obtains an expression for the LL resummation of small- x logarithms in the collinear partonic coefficient functions.

The last step of this procedure was traditionally performed in Mellin moment space, which allows to obtain rather simple analytical expressions. Despite the elegance of this result, it was soon realized that subleading effects due to the running of the strong coupling are important and should be included systematically in the resummation procedure to obtain perturbatively stable results [11, 38]. However, the inclusion of such terms in Mellin space is complicated, and not suitable for efficient numerical implementations. Recently, an alternative but equivalent formulation of the resummation was proposed [29], that solves the technical limitations of the original formulation by working directly in k_t space, leading to an efficient numerical implementation. This novel approach is at the core of the public code HELL, and allowed for a number of phenomenological applications [30, 31], including the first consistent PDF fits with small- x resummation [23–25].

So far, all HELL applications are for inclusive observables (DIS structure functions [29, 30] and the total Higgs production cross section [31]). The resummation of differential observables, of obvious interest for LHC phenomenology, has been considered in the Mellin-space formalism. Specifically, resummed expressions for rapidity distributions [32], transverse momentum distributions [33] and double differential distributions in both rapidity and transverse momentum [34] are available. It is the purpose of this section to reformulate these results in the new HELL language, thereby supplementing them with the running coupling contributions and thus providing a ready-to-use numerical implementation.

In this work, we focus on processes at hadron-hadron colliders that are gluon-gluon initiated at lowest order. These include, for instance, Higgs production, jet production, or heavy quark pair production; the latter will be considered as a practical application in Sect. 3. The reason for this choice is that the resummation is simpler, because at LL there are no collinear singularities. In other processes where the lowest order is initiated by (massless) quarks, because small- x logarithms at LL appear from chains of emissions ending with a gluon, the diagram entering the computation of the off-shell coefficient function must contain at least a gluon to (massless) quark splitting, thus producing a collinear singularity. One example is the Drell-Yan process. In such cases, the collinear singularities must be treated at the resummed level (similarly to what is done in DIS, see Ref. [30]). A study of the Drell-Yan process where this issue is addressed at differential level is left to future work [39].

Before moving to the resummation, we establish the notation by presenting the structure of differential distributions in collinear factorization for a process in proton-proton collisions. We consider a generic final-state momentum q (it can be the momentum of a single particle or the sum of momenta of different particles) in the collider center-of-mass frame, and we write the distribution differential in its invariant mass squared $Q^2 \equiv q^2$, rapidity $Y = \frac{1}{2} \log \frac{q_0^2 + q_3^2}{q_0^2 - q_3^2}$ and transverse component squared $q_t^2 = (q^1)^2 + (q^2)^2$ as

$$\begin{aligned} & \frac{d\sigma}{dQ^2 dY dq_t^2}(\tau, Q^2, Y, q_t^2) \\ &= \tau \sum_{ij} \int_{\tau}^1 \frac{dx}{x} \int dy \frac{dC_{ij}}{dQ^2 dy dq_t^2} \left(x, Q^2, y, q_t^2, \alpha_s, \frac{Q^2}{\mu_F^2} \right) \\ & \times L_{ij} \left(\frac{\tau}{x}, Y - y, \mu_F^2 \right), \end{aligned} \tag{2.1}$$

with $\tau = Q^2/s$ (s is the collider energy squared) and the sum extends over all possible partons i, j in each proton. In this expression the function

$$\frac{dC_{ij}}{dQ^2 dy dq_t^2} \left(x, Q^2, y, q_t^2, \alpha_s, \frac{Q^2}{\mu_F^2} \right) \tag{2.2}$$

is the parton-level coefficient function, which depends on $x = Q^2/\hat{s}_c$ (the parton-level analog of τ) where \hat{s}_c is the partonic center-of-mass energy,¹ and on y which is the rapidity of q with respect to the partonic center-of-mass frame, and is related to the proton-level rapidity Y by a longitudinal boost. Indeed, $Y - y$ is the rapidity of the partonic center-of-mass frame with respect to the collider frame, and it is determined by the momentum fractions \hat{x}_1, \hat{x}_2 of the partons in each proton by $Y - y = \frac{1}{2} \log \frac{\hat{x}_1}{\hat{x}_2}$. Note that we have omitted the

¹ We call it \hat{s}_c (c stands for collinear) because we will use \hat{s} for the energy squared of another system.

dependence of α_s and of the coefficient function on the renormalization scale μ_R , as such dependence is subleading in the small- x limit we are interested in. Finally, the function

$$\begin{aligned} L_{ij}(\bar{x}, \bar{y}, \mu_F^2) &= f_i(\sqrt{\bar{x}}e^{\bar{y}}, \mu_F^2) f_j(\sqrt{\bar{x}}e^{-\bar{y}}, \mu_F^2) \\ & \times \theta(e^{-2|\bar{y}|} - \bar{x}) \end{aligned} \tag{2.3}$$

is the (collinear) parton luminosity, given by the two PDFs with momentum fractions $\hat{x}_{1,2} = \sqrt{\frac{\tau}{x}}e^{\pm(Y-y)}$, and including a θ function which encodes the condition $\hat{x}_{1,2} \leq 1$.

Equation (2.1) can also be rewritten as an integral over the parton momenta \hat{x}_1, \hat{x}_2 , which represents the direct extension of the analogous formula in DIS. However, this form is more suitable for further manipulations. Indeed, it has the form of a Mellin-Fourier convolution, which implies that it can be diagonalized by taking a Mellin-Fourier transform with respect to τ and Y ,

$$\begin{aligned} & \int_0^1 d\tau \tau^{N-1} \int_{-\infty}^{\infty} dY e^{ibY} \frac{d\sigma}{dQ^2 dY dq_t^2} = \\ & \sum_{ij} \frac{dC_{ij}}{dQ^2 dy dq_t^2} \left(N, Q^2, b, q_t^2, \alpha_s, \frac{Q^2}{\mu_F^2} \right) L_{ij} \left(N, b, \mu_F^2 \right), \end{aligned} \tag{2.4}$$

where

$$\begin{aligned} & \frac{dC_{ij}}{dQ^2 dy dq_t^2} \left(N, Q^2, b, q_t^2, \alpha_s, \frac{Q^2}{\mu_F^2} \right) \\ &= \int_0^1 dx x^N \int_{-\infty}^{\infty} dy e^{iby} \\ & \times \frac{dC_{ij}}{dQ^2 dy dq_t^2} \left(x, Q^2, y, q_t^2, \alpha_s, \frac{Q^2}{\mu_F^2} \right) \\ L_{ij} \left(N, b, \mu_F^2 \right) &= \int_0^1 d\bar{x} \bar{x}^N \int_{-\infty}^{\infty} d\bar{y} e^{ib\bar{y}} L_{ij}(\bar{x}, \bar{y}, \mu_F^2) \\ &= f_i \left(N + i\frac{b}{2}, \mu_F^2 \right) f_j \left(N - i\frac{b}{2}, \mu_F^2 \right). \end{aligned} \tag{2.5}$$

In the last equality we have used the definition Eq. (2.3) and changed variable from \bar{x}, \bar{y} to $\hat{x}_{1,2} = \sqrt{\bar{x}}e^{\pm\bar{y}}$ and used explicitly the θ function to obtain the product of two Mellin transforms

$$f_i(N, \mu_F^2) = \int_0^1 d\hat{x}_{1,2} \hat{x}_{1,2}^N f_i(\hat{x}_{1,2}, \mu_F^2). \tag{2.6}$$

We further observe that the dependence on the transverse momentum does not affect the structure of the cross section formula, and thus impacts only the kinematics.

2.1 Extension of k_t factorization to differential observables in pp collisions

The works of Refs. [32–34] provide a proof of a resummation formula for differential observable at LL accuracy with fixed coupling through the so-called ladder-expansion approach. This may seem somewhat different from the original works [26–28] where the resummation is obtained by proving a k_t factorization and comparing it with the standard collinear factorization formula. In fact, despite the different languages, the two approaches are based exactly on the same underlying factorization property and lead to exactly the same result. It is thus natural to imagine that the results of Refs. [32–34] on differential distributions could be reformulated in terms of the k_t factorization approach.

Indeed, it is not difficult to follow the steps of the derivation of Refs. [32–34] and recognise the ingredients of k_t factorization to construct a factorized formula. Here, rather than repeating such a derivation, we limit ourselves to formulate the result in k_t factorization, showing that it corresponds to the results of Refs. [32–34] at LL and fixed coupling.

Similarly to the inclusive case, the differential cross section in k_t factorization turns out to be a straightforward extension of the collinear factorization Eq. (2.1) where the partons are replaced by off-shell gluons and integration over this off-shellness is added. The result reads

$$\begin{aligned} \frac{d\sigma}{dQ^2 dY dq_t^2} &= \tau \int_{\tau}^1 \frac{dz}{z} \int d\eta \int_0^\infty d\xi_1 \int_0^\infty d\xi_2 \\ &\times \frac{d\mathcal{C}}{dQ^2 d\eta dq_t^2}(z, \xi_1, \xi_2, Q^2, \eta, q_t^2, \alpha_s) \mathcal{L}\left(\frac{\tau}{z}, Y - \eta, \xi_1, \xi_2\right), \end{aligned} \tag{2.7}$$

where

$$\begin{aligned} \mathcal{L}(\bar{z}, \bar{\eta}, \xi_1, \xi_2) &= \mathcal{F}_g(\sqrt{\bar{z}}e^{\bar{\eta}}, \xi_1) \mathcal{F}_g(\sqrt{\bar{z}}e^{-\bar{\eta}}, \xi_2) \\ &\times \theta(e^{-2|\bar{\eta}|} - \bar{z}) \end{aligned} \tag{2.8}$$

and $\xi_{1,2} = \mathbf{k}_{1,2}^2/Q^2$ are the offshellness of the gluons normalized to the hard scale Q^2 , and $\mathbf{k}_{1,2}$ are the transverse components of the off-shell gluon momenta (for more details on the kinematics, see Appendix A). In the expression above $d\mathcal{C}$ is the (differential) off-shell coefficient function, representing the process-dependent hard scattering initiated by off-shell gluons. More precisely, it corresponds to the last 2GI part (in the t channel) of the amplitude squared of the process, saturating the off-shell gluon indices with a suitable projector [26–28]. Everything else is collected into the two unintegrated gluon PDFs \mathcal{F}_g , that include the standard collinear PDFs and the chain of emissions from the initial parton to the last gluon (the ladder in the language of Refs. [32–34]). The integration variables z and η are the analog of x and y of Eq. (2.1), but referred to the center-of-mass frame

of the off-shell partons. More precisely, we consider as the parton-level center-of-mass frame in k_t -factorization the one obtained if we set the off-shellness equal to zero, so that it is related to the collider frame by a longitudinal boost. More details are given in Appendix A.

We now show that Eq. (2.7) is equivalent to the result of Ref. [34].² First, we take the Mellin–Fourier transform of this expression with respect to τ and Y ,

$$\begin{aligned} &\int_0^1 d\tau \tau^{N-1} \int_{-\infty}^\infty dY e^{ibY} \frac{d\sigma}{dQ^2 dY dq_t^2} \\ &= \int_0^\infty d\xi_1 \int_0^\infty d\xi_2 \\ &\times \frac{d\mathcal{C}}{dQ^2 d\eta dq_t^2}(N, \xi_1, \xi_2, Q^2, b, q_t^2, \alpha_s) \mathcal{L}(N, b, \xi_1, \xi_2), \end{aligned} \tag{2.9}$$

with

$$\begin{aligned} &\frac{d\mathcal{C}}{dQ^2 d\eta dq_t^2}(N, \xi_1, \xi_2, Q^2, b, q_t^2, \alpha_s) \\ &= \int_0^1 dz z^N \int_{-\infty}^\infty d\eta e^{ib\eta} \\ &\times \frac{d\mathcal{C}}{dQ^2 d\eta dq_t^2}(z, \xi_1, \xi_2, Q^2, \eta, q_t^2, \alpha_s) \\ &\mathcal{L}(N, b, \xi_1, \xi_2) \\ &= \int_0^1 d\bar{z} \bar{z}^N \int_{-\infty}^\infty d\bar{\eta} e^{i b \bar{\eta}} \mathcal{L}(\bar{z}, \bar{\eta}, \xi_1, \xi_2) \\ &= \mathcal{F}_g\left(N + i\frac{b}{2}, \xi_1\right) \mathcal{F}_g\left(N - i\frac{b}{2}, \xi_2\right), \end{aligned} \tag{2.10}$$

where we have used the definition Eq. (2.8), changed variable from $\bar{z}, \bar{\eta}$ to $x_{1,2} = \sqrt{\bar{z}}e^{\pm\bar{\eta}}$ (the longitudinal proton’s momentum fractions carried by each off-shell gluon) and used the θ function to obtain the product of two Mellin transforms

$$\mathcal{F}_g(N, \xi) = \int_0^1 dx_{1,2} x_{1,2}^N \mathcal{F}_g(x_{1,2}, \xi). \tag{2.11}$$

At this point we follow Ref. [26–28] to write the unintegrated PDF as

$$\begin{aligned} \mathcal{F}_g(N, \xi) &= R(N, \alpha_s) \gamma(N, \alpha_s) \left(\frac{Q^2}{\mu_F^2}\right)^{\gamma(N, \alpha_s)} \\ &\times \xi^{\gamma(N, \alpha_s)-1} f_g(N, \mu_F^2), \end{aligned} \tag{2.12}$$

where $\gamma(N, \alpha_s)$ is the resummed (gluon) anomalous dimension at LL and $R(N, \alpha_s)$ is a scheme dependent factor. Note

² Notice that Ref. [34] considers only the double differential distribution in rapidity and transverse momentum, because it focusses on the Higgs production process, where the invariant mass is clearly fixed to the Higgs mass. However, the derivation there is general enough to be valid also for invariant mass distributions.

that we are ignoring quark contributions for simplicity (we will discuss quarks later in Sect. 2.3). Plugging Eq. (2.12) into Eq. (2.9) we immediately recover the result of Ref. [34]. Integrating over q_t^2 we also reproduce the result of Ref. [32].

To reproduce the result of Ref. [33], which is not differential in rapidity, it is simpler to integrate Eq. (2.7) over Y and then take simply a Mellin transform before using Eq. (2.12). The first step leads to

$$\frac{d\sigma}{dQ^2 dq_t^2} = \tau \int_{\tau}^1 \frac{dz}{z} \int_0^{\infty} d\xi_1 \int_0^{\infty} d\xi_2 \times \frac{dC}{dQ^2 dq_t^2}(z, \xi_1, \xi_2, Q^2, q_t^2, \alpha_s) \mathcal{L}\left(\frac{\tau}{z}, \xi_1, \xi_2\right), \quad (2.13)$$

with

$$\begin{aligned} \mathcal{L}(\bar{z}, \xi_1, \xi_2) &= \int d\bar{\eta} \mathcal{F}_g(\sqrt{\bar{z}}e^{\bar{\eta}}, \xi_1) \mathcal{F}_g(\sqrt{\bar{z}}e^{-\bar{\eta}}, \xi_2) \theta(e^{-2|\bar{\eta}|} - \bar{z}) \\ &= \int_{\bar{z}}^1 dx_2 \mathcal{F}_g\left(\frac{\bar{z}}{x_2}, \xi_1\right) \mathcal{F}_g(x_2, \xi_2). \end{aligned} \quad (2.14)$$

Because this new rapidity-integrated luminosity has the form of a Mellin convolution, after taking a Mellin transform of the cross section we get

$$\int_0^1 d\tau \tau^{N-1} \frac{d\sigma}{dQ^2 dq_t^2} = \int_0^{\infty} d\xi_1 \int_0^{\infty} d\xi_2 \frac{dC}{dQ^2 dq_t^2} \times (N, \xi_1, \xi_2, Q^2, q_t^2, \alpha_s) \mathcal{F}_g(N, \xi_1) \mathcal{F}_g(N, \xi_2), \quad (2.15)$$

with

$$\begin{aligned} \frac{dC}{dQ^2 dq_t^2}(N, \xi_1, \xi_2, Q^2, q_t^2, \alpha_s) \\ = \int_0^1 dz z^N \frac{dC}{dQ^2 dq_t^2}(z, \xi_1, \xi_2, Q^2, q_t^2, \alpha_s). \end{aligned} \quad (2.16)$$

Plugging now Eq. (2.12) into Eq. (2.15) we finally obtain the result of Ref. [33].

Because the unintegrated PDF depends on ξ through $\xi^{\gamma-1}$, the integrals over $\xi_{1,2}$ take the form of Mellin transforms. Therefore, the results above can be expressed (up to factors) as the γ 'th Mellin moments with respect to $\xi_{1,2}$ of the partonic off-shell coefficient functions, usually called impact factors. These results can be further supplemented with running coupling effects as described in Refs. [11,38]. However, as anticipated, adding running coupling effects to the impact factors is not suitable for numerical implementation. In the next section we will start again from Eq. (2.7) to construct a resummed expression at differential level in the HELL language, which makes the inclusion of running coupling effects straightforward and leads to a stable numerical implementation.

2.2 Small- x resummation of differential distributions in the HELL language

The main advantage of the formulation of small- x resummation of Refs. [29–31] used in the HELL code is the much simpler and reliable numerical implementation. The reason is twofold. On the one hand, the inclusion of running coupling effects in the resummation can be done straightforwardly without approximation and without affecting the numerical performance, as opposed to the impact-factor approach of Refs. [11,38] where it leads to a divergent series that has to be treated in an approximate way. On the other hand, the result can be expressed in terms of the off-shell coefficient function directly in momentum space, as opposed to the impact-factor formulation where a double Mellin transform in both z and ξ is required for each initial-state off-shell gluon. If these Mellin transforms can be computed analytically, the (very minor) price to pay of the HELL formulation is that the ξ integration has to be performed numerically. However, when the Mellin transform in ξ cannot be computed analytically, the impact-factor formulation becomes problematic, while in the HELL approach this does not represent a problem.

The key step of the HELL approach is to write the unintegrated PDF in terms of the collinear gluon and quark-singlet PDFs in a way that includes running coupling effects. The generic form of such an expression, valid at least at LL, is [29–31]

$$\begin{aligned} \mathcal{F}_g(N, \xi) &= U'(N, Q^2\xi, \mu_F^2) f_g(N, \mu_F^2) \\ &+ \frac{C_F}{C_A} \left[U'(N, Q^2\xi, \mu_F^2) - \delta(\xi) \right] f_q(N, \mu_F^2), \end{aligned} \quad (2.17)$$

where

$$U'(N, Q^2\xi, \mu_F^2) \equiv \frac{d}{d\xi} U(N, Q^2\xi, \mu_F^2) \quad (2.18)$$

and $U(N, \mathbf{k}^2, \mu_F^2)$ is the evolution function of the collinear gluon³ from the scale μ_F^2 to the scale \mathbf{k}^2 , times the scheme dependent function $R(N, \alpha_s)$. In other words, $U(N, \mathbf{k}^2, \mu_F^2)$ is the solution of the DGLAP equation using the small- x LL anomalous dimension, which involves only gluons (they do not mix with the quarks at LL). Keeping running coupling effects when solving the DGLAP evolution equation provides the necessary ingredient to include the sought running coupling effects in the resummation [29–31]. Conversely, evaluating the evolution function at fixed-coupling we get back Eq. (2.12).

³ It is worth noting that the quark part of (2.17) uses the same evolver of the gluon part. This is justified as, in the $x \rightarrow 0$ limit, the leading splitting functions, P_{gg} and P_{gq} , are identical up to a factor $\frac{C_F}{C_A}$. The subtraction of the $\delta(\xi)$ in the quark part, that represents the no-splitting event in which the parton remains collinear, is required as the first splitting of the quark into a gluon must be present, and so that contribution must start at order α_s .

In practice, to simplify the numerical implementation and avoid potential numerical issues, the evolution function is approximated in a way that reproduces exactly the results of Refs. [11, 38], namely it is valid at LL and at “leading running coupling” (i.e. leading β_0 terms are retained). Within this approximation it takes the form [30, 31]

$$U(N, Q^2\xi, \mu_F^2) \simeq R(N, \alpha_s) D_{\text{higher-twist}}\left(\frac{Q^2}{\mu_F^2}\xi\right) \times U_{\text{ABF}}\left(N, \frac{Q^2}{\mu_F^2}\xi\right), \tag{2.19}$$

where

$$D_{\text{higher-twist}}(\xi) = \begin{cases} 1 & \xi \geq 1 \\ 1 - (-\alpha_s\beta_0 \log \xi)^{1+\frac{1}{\alpha_s\beta_0}} & \xi_0 < \xi < 1 \\ 0 & \xi \leq \xi_0, \end{cases} \tag{2.20}$$

$$\xi_0 = \exp\frac{-1}{\alpha_s\beta_0},$$

is a damping function at small ξ , designed to keep unaffected the perturbative expansion of the evolution function while ensuring that it vanishes at the Landau pole ξ_0 as it would do at LL with full running coupling [30], and

$$U_{\text{ABF}}(N, \xi) = \left(1 + r(N, \alpha_s) \log \xi\right)^{\frac{\gamma(N, \alpha_s)}{r(N, \alpha_s)}},$$

$$r(N, \alpha_s) = \alpha_s^2 \beta_0 \frac{d}{d\alpha_s} \log[\gamma(N, \alpha_s)], \tag{2.21}$$

is the approximated evolution function. The anomalous dimension γ appearing above is in principle the LL anomalous dimension. However, it is convenient to include subleading contributions in it that simply produce subleading effects in the resummation but make the result consistent with the resummation in DGLAP evolution. As this discussion is not central for the present work, we refer the Reader to Ref. [31] for further detail. In the numerical implementation, we will ignore the scheme factor $R(N, \alpha_s)$. The reason is that we use to perform small- x resummation in the so-called $Q_0\overline{\text{MS}}$ scheme [28, 36, 40, 41] where by definition $R(N, \alpha_s) = 1$. This scheme differs from the usual $\overline{\text{MS}}$ scheme at relative order α_s^3 (at LL), and therefore it can be safely used in conjunction with $\overline{\text{MS}}$ fixed-order computations up to NNLO.

Let us focus for simplicity on the gluon contribution only, thus neglecting the quark term in Eq. (2.17). Plugging Eq. (2.17) into Eq. (2.9) we get

$$\int_0^1 d\tau \tau^{N-1} \int_{-\infty}^{\infty} dY e^{ibY} \frac{d\sigma}{dQ^2 dY dq_t^2}$$

$$= \int_0^{\infty} d\xi_1 \int_0^{\infty} d\xi_2 \frac{dC}{dQ^2 d\eta dq_t^2}(N, \xi_1, \xi_2, Q^2, b, q_t^2, \alpha_s)$$

$$\times U'\left(N + i\frac{b}{2}, Q^2\xi_1, \mu_F^2\right) f_g\left(N + i\frac{b}{2}, \mu_F^2\right)$$

$$\times U'\left(N - i\frac{b}{2}, Q^2\xi_2, \mu_F^2\right) f_g\left(N - i\frac{b}{2}, \mu_F^2\right). \tag{2.22}$$

Comparing this expression with the gluon–gluon channel of the collinear factorization expression Eq. (2.4) and Eq. (2.5) we find the identification

$$\frac{dC_{gg}}{dQ^2 dy dq_t^2}\left(N, Q^2, b, q_t^2, \alpha_s, \frac{Q^2}{\mu_F^2}\right)$$

$$= \int_0^{\infty} d\xi_1 \int_0^{\infty} d\xi_2 \frac{dC}{dQ^2 d\eta dq_t^2}(N, \xi_1, \xi_2, Q^2, b, q_t^2, \alpha_s)$$

$$\times U'\left(N + i\frac{b}{2}, Q^2\xi_1, \mu_F^2\right) U'\left(N - i\frac{b}{2}, Q^2\xi_2, \mu_F^2\right). \tag{2.23}$$

So far this is not dissimilar to the approach of older works; in particular, if one replaces U' with the LL fixed-coupling expression from Eq. (2.12) one recognises the definition of the impact factor. Here instead, we keep a more generic expression for U' and further manipulate the result. Indeed, we notice that the N, b dependence of the right-hand side of Eq. (2.23) has the same form of the right-hand side of Eq. (2.4) or Eq. (2.9). We thus recognise Eq. (2.23) as the Mellin-Fourier transform of

$$\frac{dC_{gg}}{dQ^2 dy dq_t^2}\left(x, Q^2, y, q_t^2, \alpha_s, \frac{Q^2}{\mu_F^2}\right)$$

$$= \int_0^{\infty} d\xi_1 \int_0^{\infty} d\xi_2 \int_x^1 \frac{dz}{z} \int_{-\frac{1}{2}\log\frac{x}{z}}^{\frac{1}{2}\log\frac{x}{z}} d\bar{\eta}$$

$$\times \frac{dC}{dQ^2 d\eta dq_t^2}(z, \xi_1, \xi_2, Q^2, y - \bar{\eta}, q_t^2, \alpha_s)$$

$$\times U'\left(\sqrt{\frac{x}{z}}e^{\bar{\eta}}, Q^2\xi_1, \mu_F^2\right) U'\left(\sqrt{\frac{x}{z}}e^{-\bar{\eta}}, Q^2\xi_2, \mu_F^2\right), \tag{2.24}$$

which is expressed as a 4-dimensional integral (to be performed numerically in general) over simple quantities, namely the differential off-shell coefficient function and the evolution factors in physical momentum space. This result is very convenient from a numerical point of view. The two additional integrations over z and η are much simpler to compute than the inverse Mellin-Fourier transform over N and b of Eq. (2.23), especially in HELL, because the anomalous dimension appearing in the definition of U' is available in HELL only for values of N along a specific inversion contour, which would not be sufficient here due to the $\pm ib$ imaginary shift. Instead, because the evolution function U is universal (process independent), it is computed once and for all in HELL directly in momentum space, and it can be easily used in an expression like Eq. (2.24). Moreover, as already mentioned, with respect to the impact-factor formulation this result easily incorporates the running coupling contributions through the use of the proper evolution function U , Eq. (2.19).

We want to emphasize a difference with respect to previous formulations of resummation in the HELL language. In previous works, because the N dependence of the off-shell coefficient function is subleading, we used to set $N = 0$ in it before computing the inverse Mellin transform. The main motivation was that the analytical expressions obtained in this way were simpler, and in some cases it is not possible to compute the Mellin transform of the off-shell coefficient function analytically for generic N , but it is possible for $N = 0$. In our case, this approach would correspond to setting $N = 0$ in the off-shell coefficient function in Eq. (2.23) before computing the inverse Mellin-Fourier transform. However, when dealing with differential distribution we are often not able to compute analytically the Mellin transform of the off-shell coefficient function, not even in $N = 0$. So there would be no advantage in setting $N = 0$ in it. Conversely, there would be disadvantages. Indeed, some physical kinematic constraints would be approximated if computed in $N = 0$. One of the consequences is that the endpoint of the rapidity distribution, which is a physical property of the process determined by its kinematics, would be wrong when setting $N = 0$. This is not dissimilar to what has been found in Ref. [30] in the case of DIS, where quark mass effects on kinematic constraints were lost when setting $N = 0$, requiring a restoration of the constraints by hand. Here, we thus decide that it is much better (and simpler) to keep the subleading N dependence, thereby preserving physical kinematic constraints, without paying any price from the numerical point of view.

2.3 All partonic channels

In the resummed expression Eq. (2.24) the key ingredient is (the ξ -derivative of) the evolution function in x space,⁴ computed in HELL as the inverse Mellin transform of Eq. (2.19). We observe that such inverse Mellin transform is a distribution. Indeed, expanding $U(N, Q^2\xi, \mu_F^2)$ in powers of α_s , the zeroth order term is just 1, whose inverse Mellin is $\delta(1 - x)$. Since this is the only distributional contribution in U , we find it more convenient to write it explicitly,

$$\begin{aligned}
 U(N, Q^2\xi, \mu_F^2) &= 1 + U_{\text{reg}}(N, Q^2\xi, \mu_F^2) \\
 \Updownarrow \\
 U(x, Q^2\xi, \mu_F^2) &= \delta(1 - x) + U_{\text{reg}}(x, Q^2\xi, \mu_F^2), \quad (2.25)
 \end{aligned}$$

where U_{reg} is an ordinary function. Computing the ξ -derivative appearing in Eq. (2.17) is not entirely trivial. To do so we first introduce explicitly a factor $\theta(\xi)$ in the definition of the evolution function, $U(N, Q^2\xi, \mu_F^2) =$

$\theta(\xi) [1 + U_{\text{reg}}(N, Q^2\xi, \mu_F^2)]$, which is conceptually harmless as certainly the scale $Q^2\xi = \mathbf{k}^2$ has to be positive. When deriving we get

$$\begin{aligned}
 U'(N, Q^2\xi, \mu_F^2) &= \delta(\xi) + \delta(\xi)U_{\text{reg}}(N, 0, \mu_F^2) \\
 &\quad + \theta(\xi)U'_{\text{reg}}(N, Q^2\xi, \mu_F^2) \\
 &= \delta(\xi) - \delta(\xi) \int_0^{\frac{\mu_F^2}{Q^2}} d\xi' U'_{\text{reg}}(N, Q^2\xi', \mu_F^2) \\
 &\quad + \theta(\xi)U'_{\text{reg}}(N, Q^2\xi, \mu_F^2) \\
 &= \delta(\xi) + \left[U'_{\text{reg}}(N, Q^2\xi, \mu_F^2) \right]_+ \quad (2.26)
 \end{aligned}$$

where in the second step we have used the fact that $U_{\text{reg}}(N, \mu_F^2, \mu_F^2) = 0$ and in the last step we have defined the plus distribution according to

$$\begin{aligned}
 \int_0^\infty d\xi f(\xi) [g(\xi)]_+ &= \int_0^{\frac{\mu_F^2}{Q^2}} d\xi [f(\xi) - f(0)] g(\xi) \\
 &\quad + \int_{\frac{\mu_F^2}{Q^2}}^\infty d\xi f(\xi) g(\xi). \quad (2.27)
 \end{aligned}$$

The $\delta(\xi)$ term appearing as the derivative of the zeroth order of the evolution has a precise physical meaning: it represents the undisturbed gluon, that does not emit and thus it remains on-shell ($\xi = 0$). This indeed corresponds to the term subtracted in the quark contribution to the unintegrated PDF, Eq. (2.17).

We now observe that the introduction of the plus distribution is not really necessary, because the contribution $U_{\text{reg}}(N, 0, \mu_F^2)$ appearing in the first line of Eq. (2.26) is finite. More precisely, because $U(N, 0, \mu_F^2) = 0$ by construction, Eq. (2.19), we have $U_{\text{reg}}(N, 0, \mu_F^2) = -1$, corresponding in x -space to

$$U_{\text{reg}}(x, 0, \mu_F^2) = -\delta(1 - x). \quad (2.28)$$

If this is the case, the first two terms in the first line of Eq. (2.26) would cancel, thus leaving the simpler result $U'(N, Q^2\xi, \mu_F^2) = U'_{\text{reg}}(N, Q^2\xi, \mu_F^2)$ which is what we would have obtained if we hadn't introduced the θ function. This implies that the nice physical distinction between the no-emission contribution $\delta(\xi)$ and the at-least-one-emission contribution $U'_{\text{reg}}(N, Q^2\xi, \mu_F^2)$ gets lost. This is clearly undesirable, and may hint at a problem in the construction of the evolution function.

To understand and overcome this problem, we observe that the $\xi \rightarrow 0$ limit of U'_{reg} , Eq. (2.28), is localised at large x . But the evolution function at large x is not expected to be accurate, as it is constructed to resum logarithmic contributions at small x . Therefore, we can (and we do) damp the function $U_{\text{reg}}(x, Q^2\xi, \mu_F^2)$ (and thus its ξ -derivative) at large x , with a damping function of the form $(1 - x)^a$ (we use

⁴ As we are running out of letters, we are now using x for the generic first argument of the evolution function in momentum space, not to be confused with the variable $x = Q^2/\hat{s}_c$ which is the argument of the collinear coefficient function.

$a = 2$ in the code). After damping, the evolution function satisfies

$$U_{\text{reg}}(x = 1, Q^2\xi, \mu_F^2) = 0, \tag{2.29}$$

for any value of ξ , including $\xi = 0$. In this way, we obtain $U_{\text{reg}}(x, 0, \mu_F^2) = 0$ and thus $U_{\text{reg}}(N, 0, \mu_F^2) = 0$, implying that the second term in the first line of Eq. (2.26) vanishes, thus giving

$$U'(N, Q^2\xi, \mu_F^2) = \delta(\xi) + U'_{\text{reg}}(N, Q^2\xi, \mu_F^2) \\ \Downarrow \\ U'(x, Q^2\xi, \mu_F^2) = \delta(\xi)\delta(1-x) + U'_{\text{reg}}(x, Q^2\xi, \mu_F^2). \tag{2.30}$$

In other words, because of the large- x damping, the plus distribution is ineffective. For completeness, we have verified that the numerical integral of $U'_{\text{reg}}(x, Q^2\xi, \mu_F^2)$ from zero to μ_F^2/Q^2 gives indeed zero for all values of x .

Let us now come back to the resummed coefficient function. According to Eq. (2.30), the unintegrated PDF Eq. (2.17) can be rewritten as

$$\mathcal{F}_g(N, \xi) = \left[U'_{\text{reg}}(N, Q^2\xi, \mu_F^2) + \delta(\xi) \right] f_g(N, \mu_F^2) \\ + \frac{C_F}{C_A} U'_{\text{reg}}(N, Q^2\xi, \mu_F^2) f_q(N, \mu_F^2). \tag{2.31}$$

Physically, the $\delta(\xi)$ contribution in the equation above represents the (on-shell) gluon that does not emit, thus producing no logs: this is the fixed-order contribution, and it reproduces the on-shell result. The other term, U'_{reg} , is the term containing at least one emission, and thus at least one small- x log.

Starting from Eq. (2.31) and proceeding as in the previous section, keeping also the quark contributions this time, we obtain the following expressions

$$\frac{dC_{gg}}{dQ^2 dy dq_t^2} \left(x, Q^2, y, q_t^2, \alpha_s, \frac{Q^2}{\mu_F^2} \right) = \int_0^\infty d\xi_1 \int_0^\infty d\xi_2 \int_x^1 \frac{dz}{z} \int_{-\frac{1}{2} \log \frac{z}{x}}^{\frac{1}{2} \log \frac{z}{x}} d\bar{\eta} \frac{dC}{dQ^2 d\eta dq_t^2} (z, \xi_1, \xi_2, Q^2, y - \bar{\eta}, q_t^2, \alpha_s) \\ \times \left[U'_{\text{reg}} \left(\sqrt{\frac{x}{z}} e^{\bar{\eta}}, Q^2\xi_1, \mu_F^2 \right) + \delta(\xi_1)\delta \left(1 - \sqrt{\frac{x}{z}} e^{\bar{\eta}} \right) \right] \left[U'_{\text{reg}} \left(\sqrt{\frac{x}{z}} e^{-\bar{\eta}}, Q^2\xi_2, \mu_F^2 \right) + \delta(\xi_2)\delta \left(1 - \sqrt{\frac{x}{z}} e^{-\bar{\eta}} \right) \right], \tag{2.32a}$$

$$\frac{dC_{qg}}{dQ^2 dy dq_t^2} \left(x, Q^2, y, q_t^2, \alpha_s, \frac{Q^2}{\mu_F^2} \right) = \frac{C_F}{C_A} \int_0^\infty d\xi_1 \int_0^\infty d\xi_2 \int_x^1 \frac{dz}{z} \int_{-\frac{1}{2} \log \frac{z}{x}}^{\frac{1}{2} \log \frac{z}{x}} d\bar{\eta} \\ \times \frac{dC}{dQ^2 d\eta dq_t^2} (z, \xi_1, \xi_2, Q^2, y - \bar{\eta}, q_t^2, \alpha_s) \\ \times U'_{\text{reg}} \left(\sqrt{\frac{x}{z}} e^{\bar{\eta}}, Q^2\xi_1, \mu_F^2 \right) \left[U'_{\text{reg}} \left(\sqrt{\frac{x}{z}} e^{-\bar{\eta}}, Q^2\xi_2, \mu_F^2 \right) + \delta(\xi_2)\delta \left(1 - \sqrt{\frac{x}{z}} e^{-\bar{\eta}} \right) \right], \tag{2.32b}$$

$$\frac{dC_{gq}}{dQ^2 dy dq_t^2} \left(x, Q^2, y, q_t^2, \alpha_s, \frac{Q^2}{\mu_F^2} \right) = \frac{C_F}{C_A} \int_0^\infty d\xi_1 \int_0^\infty d\xi_2 \int_x^1 \frac{dz}{z} \int_{-\frac{1}{2} \log \frac{z}{x}}^{\frac{1}{2} \log \frac{z}{x}} d\bar{\eta} \\ \times \frac{dC}{dQ^2 d\eta dq_t^2} (z, \xi_1, \xi_2, Q^2, y - \bar{\eta}, q_t^2, \alpha_s) \\ \times \left[U'_{\text{reg}} \left(\sqrt{\frac{x}{z}} e^{\bar{\eta}}, Q^2\xi_1, \mu_F^2 \right) + \delta(\xi_1)\delta \left(1 - \sqrt{\frac{x}{z}} e^{\bar{\eta}} \right) \right] U'_{\text{reg}} \left(\sqrt{\frac{x}{z}} e^{-\bar{\eta}}, Q^2\xi_2, \mu_F^2 \right), \tag{2.32c}$$

$$\frac{dC_{qq}}{dQ^2 dy dq_t^2} \left(x, Q^2, y, q_t^2, \alpha_s, \frac{Q^2}{\mu_F^2} \right) = \left(\frac{C_F}{C_A} \right)^2 \int_0^\infty d\xi_1 \int_0^\infty d\xi_2 \int_x^1 \frac{dz}{z} \int_{-\frac{1}{2} \log \frac{z}{x}}^{\frac{1}{2} \log \frac{z}{x}} d\bar{\eta} \\ \times \frac{dC}{dQ^2 d\eta dq_t^2} (z, \xi_1, \xi_2, Q^2, y - \bar{\eta}, q_t^2, \alpha_s) \\ \times U'_{\text{reg}} \left(\sqrt{\frac{x}{z}} e^{\bar{\eta}}, Q^2\xi_1, \mu_F^2 \right) U'_{\text{reg}} \left(\sqrt{\frac{x}{z}} e^{-\bar{\eta}}, Q^2\xi_2, \mu_F^2 \right). \tag{2.32d}$$

These results can be written in a more compact form as

$$\frac{dC_{gg}}{dQ^2 dy dq_t^2} = \frac{dC_{reg}}{dQ^2 dy dq_t^2} + \frac{dC_{aux+}}{dQ^2 dy dq_t^2} + \frac{dC_{aux-}}{dQ^2 dy dq_t^2} + \frac{dC}{dQ^2 d\eta dq_t^2}(x, 0, 0, Q^2, y, q_t^2, \alpha_s), \tag{2.33a}$$

$$\frac{dC_{qg}}{dQ^2 dy dq_t^2} = \frac{C_F}{C_A} \left[\frac{dC_{reg}}{dQ^2 dy dq_t^2} + \frac{dC_{aux+}}{dQ^2 dy dq_t^2} \right], \tag{2.33b}$$

$$\frac{dC_{gq}}{dQ^2 dy dq_t^2} = \frac{C_F}{C_A} \left[\frac{dC_{reg}}{dQ^2 dy dq_t^2} + \frac{dC_{aux-}}{dQ^2 dy dq_t^2} \right], \tag{2.33c}$$

$$\frac{dC_{qq}}{dQ^2 dy dq_t^2} = \left(\frac{C_F}{C_A} \right)^2 \frac{dC_{reg}}{dQ^2 dy dq_t^2} \tag{2.33d}$$

having defined

$$\frac{dC_{reg}}{dQ^2 dy dq_t^2} \left(x, Q^2, y, q_t^2, \alpha_s, \frac{Q^2}{\mu_F^2} \right) = \int_0^\infty d\xi_1 \int_0^\infty d\xi_2 \int_x^1 \frac{dz}{z} \int_{-\frac{1}{2} \log \frac{x}{z}}^{\frac{1}{2} \log \frac{x}{z}} d\bar{\eta} \times \frac{dC}{dQ^2 d\eta dq_t^2}(z, \xi_1, \xi_2, Q^2, y - \bar{\eta}, q_t^2, \alpha_s) U'_{reg} \left(\sqrt{\frac{x}{z}} e^{\bar{\eta}}, Q^2 \xi_1, \mu_F^2 \right) U'_{reg} \left(\sqrt{\frac{x}{z}} e^{-\bar{\eta}}, Q^2 \xi_2, \mu_F^2 \right) \tag{2.34}$$

and

$$\frac{dC_{aux\pm}}{dQ^2 dy dq_t^2} \left(x, Q^2, y, q_t^2, \alpha_s, \frac{Q^2}{\mu_F^2} \right) = \int_0^\infty d\xi \int_x^1 \frac{dz}{z} \frac{dC}{dQ^2 d\eta dq_t^2} \left(z, \xi, 0, Q^2, y \pm \frac{1}{2} \log \frac{z}{x}, q_t^2, \alpha_s \right) U'_{reg} \left(\frac{x}{z}, Q^2 \xi, \mu_F^2 \right), \tag{2.35}$$

where in the last equation we have used the symmetry $\xi_1 \leftrightarrow \xi_2$ of the off-shell coefficient. So in conclusion the resummed expressions for all channels are written in terms of a “regular” resummed coefficient and two simpler “auxiliary” functions,⁵ each defined in terms of integrals over ordinary functions (and thus easy to implement numerically). The gg coefficient function also depends on the on-shell limit of the off-shell coefficient; however, whenever the resummed result is matched to a fixed-order computation, this contribution will be subtracted and thus in practical applications it will never be needed.

We observe that the auxiliary functions are obtained by putting on shell one of the incoming gluons. Therefore, they represent a contribution in which resummation, obtained from k_t factorization, acts on a single initial state parton, while the other obeys the standard collinear factorization. This resembles the hybrid factorization discussed in Refs. [42–47] and used to describe forward production. We believe that our auxiliary contribution does indeed represent the same resummed contributions obtained from the hybrid factoriza-

tion. However, there may be some differences due to the different approaches to resummation, that we aim at investigating in a future work.

2.4 Matching to fixed order

The resummed result Eq. (2.32) contains only the small- x logarithms. For phenomenological applications, it has to be matched with a fixed-order computation. To do this, we need to compute its expansion in powers of α_s up to some order, subtract it and replace it with the exact fixed-order result at the same order.

Computing the α_s expansion of the resummed result is in principle straightforward, but it needs some care in practice as we shall now see. Note that the α_s dependence comes fully

from the integrand of Eq. (2.32), and specifically from the evolution function U'_{reg} , as the off-shell coefficient function is needed only at the lowest non-trivial order to achieve LL accuracy. To construct the expansion of U'_{reg} , let us consider the expansion of U_{reg} first. Because of Eqs. (2.19) and (2.21), it is clear that such an expansion contains powers of $\log \xi$. The first couple of orders take the form (in both the \overline{MS} and $Q_0\overline{MS}$ schemes)

$$U_{reg}(N, Q^2 \xi, \mu_F^2) = \alpha_s (\mu_F^2) \gamma_0(N) \log \frac{Q^2 \xi}{\mu_F^2} + \alpha_s^2 (\mu_F^2) \left[\gamma_1(N) \log \frac{Q^2 \xi}{\mu_F^2} + \frac{1}{2} \gamma_0(N) \times (\gamma_0(N) - \beta_0) \log^2 \frac{Q^2 \xi}{\mu_F^2} \right] + \mathcal{O}(\alpha_s^3), \tag{2.36}$$

having assumed the expansion $\gamma(N, \alpha_s) = \alpha_s \gamma_0 + \alpha_s^2 \gamma_1 + \mathcal{O}(\alpha_s^3)$ for the resummed anomalous dimension (see Refs. [31, 48] for explicit expressions). After computing the derivative with respect to ξ , terms of the form $\log^k \xi / \xi$ appear. Such

⁵ The name “auxiliary” follows the nomenclature introduced in Ref. [31], extended to differential distributions.

terms are not integrable in the $\xi \rightarrow 0$ limit, and thus require a regularization procedure.

To do so, we recall that the actual form of the derivative of the evolution function has a plus distribution around U'_{reg} , Eq. (2.26). The plus distribution does not play a role at resummed level because to all orders $U'_{\text{reg}}(N, 0, \mu_F^2) = 0$, but this is not true order by order. The order by order expansion

having defined $P_{00}(x)$ as the Mellin convolution of two P_0 's, and having used the expansion $P(x, \alpha_s) = \alpha_s P_0(x) + \alpha_s^2 P_1(x) + \mathcal{O}(\alpha_s^3)$ which is the inverse Mellin transform of the resummed anomalous dimension $\gamma(N, \alpha_s)$.

Plugging these expansions into Eq. (2.34) and Eq. (2.35) we finally obtain the sought perturbative expansion of the resummed result. In particular, we find up to relative $\mathcal{O}(\alpha_s^2)$

$$\frac{dC_{\text{reg}}}{dQ^2 dy dq_t^2} \left(x, Q^2, y, q_t^2, \alpha_s, \frac{Q^2}{\mu_F^2} \right) = \int_0^\infty d\xi_1 \int_0^\infty d\xi_2 \int_x^1 \frac{dz}{z} \int_{-\frac{1}{2} \log \frac{z}{x}}^{\frac{1}{2} \log \frac{z}{x}} d\bar{\eta} \times \frac{dC}{dQ^2 d\eta dq_t^2} (z, \xi_1, \xi_2, Q^2, y - \bar{\eta}, q_t^2, \alpha_s) \left[\alpha_s^2(\mu_F^2) \left(\frac{1}{\xi_1} \right)_+ \left(\frac{1}{\xi_2} \right)_+ P_0 \left(\sqrt{\frac{x}{z}} e^{\bar{\eta}} \right) P_0 \left(\sqrt{\frac{x}{z}} e^{-\bar{\eta}} \right) + \mathcal{O}(\alpha_s^3) \right] \tag{2.39}$$

$$\frac{dC_{\text{aux}\pm}}{dQ^2 dy dq_t^2} \left(x, Q^2, y, q_t^2, \alpha_s, \frac{Q^2}{\mu_F^2} \right) = \int_0^\infty d\xi \int_x^1 \frac{dz}{z} \frac{dC}{dQ^2 d\eta dq_t^2} \times \left(z, \xi, 0, Q^2, y \pm \frac{1}{2} \log \frac{z}{x}, q_t^2, \alpha_s \right) \left\{ \alpha_s(\mu_F^2) P_0 \left(\frac{x}{z} \right) \left(\frac{1}{\xi} \right)_+ + \alpha_s^2(\mu_F^2) \left[P_1 \left(\frac{x}{z} \right) \left(\frac{1}{\xi} \right)_+ + \left(P_{00} \left(\frac{x}{z} \right) - \beta_0 P_0 \left(\frac{x}{z} \right) \right) \left(\frac{\log \frac{Q^2 \xi}{\mu_F^2}}{\xi} \right)_+ \right] + \mathcal{O}(\alpha_s^3) \right\} \tag{2.40}$$

sion of the evolution function diverges at $\xi = 0$, and so the plus distribution becomes essential.

With a slight abuse of notation,⁶ starting from Eq. (2.36), we can write the first couple of orders of the expansion of U'_{reg} ,

$$U'_{\text{reg}}(N, Q^2 \xi, \mu_F^2) = \alpha_s(\mu_F^2) \gamma_0(N) \left(\frac{1}{\xi} \right)_+ + \alpha_s^2(\mu_F^2) \left[\gamma_1(N) \left(\frac{1}{\xi} \right)_+ + \gamma_0(N) (\gamma_0(N) - \beta_0) \times \left(\frac{\log \frac{Q^2 \xi}{\mu_F^2}}{\xi} \right)_+ \right] + \mathcal{O}(\alpha_s^3), \tag{2.37}$$

or, in x space,

$$U'_{\text{reg}}(x, Q^2 \xi, \mu_F^2) = \alpha_s(\mu_F^2) P_0(x) \left(\frac{1}{\xi} \right)_+ + \alpha_s^2(\mu_F^2) \left[P_1(x) \left(\frac{1}{\xi} \right)_+ \times + (P_{00}(x) - \beta_0 P_0(x)) \times \left(\frac{\log \frac{Q^2 \xi}{\mu_F^2}}{\xi} \right)_+ \right] + \mathcal{O}(\alpha_s^3), \tag{2.38}$$

out of which we can construct the expansion of each coefficient function through Eq. (2.33).

We note in conclusion that this procedure is not dissimilar to what was used in previous works, see e.g. Ref. [31], where the expansion was obtained by expanding the impact factor. However, the derivation obtained here is more “direct”, and the result is written in a form that is immediately usable to compute the expansion numerically, without the need to compute analytically the impact factor.

3 Heavy-quark pair production

Having described the general formalism for the small- x resummation of differential distributions in HELL, we now focus on a specific process: heavy-quark pair production in proton–proton collisions. This process is relevant because at the LHC, and in particular at LHCb, it is measured in the forward region where one parton is at small x , and it can thus provide important constraints on the PDFs (the gluon in particular) in a region of x that is so far unexplored. Moreover, NLO results for this process are available [49,50], and NNLO corrections have also been computed recently [51], making this process suitable for precision studies.

The process can be schematized as

$$p(P_1) + p(P_2) \rightarrow Q(p) + \bar{Q}(\bar{p}) + X, \tag{3.1}$$

⁶ The most correct way of writing these results is to keep the plus distribution around U'_{reg} everywhere.

where the two incoming protons have light-cone momenta $P_{1,2}$ with $(P_1 + P_2)^2 = s$, the outgoing heavy quarks have mass m and momenta p, \bar{p} with $p^2 = \bar{p}^2 = m^2$, and X represents any additional radiation together with the remnants of the protons. For simplicity, we consider the final state to be given by the heavy quarks themselves, thus ignoring their hadronization and eventual decay into lighter hadrons.⁷ These effects should not affect the impact of resummation, as they factorize (at least at LL) with respect to the hard scattering process. A full phenomenological study of the process including these effects is beyond the scope of this paper and is left to future work. Rather, the scope of this section is to demonstrate the application of the framework introduced in this paper.

The resummation of high-energy logarithms in heavy quark pair production has been considered in the literature, both at the level of the total cross section [27, 52] and for some differential observables [45, 46, 53–55]. To perform small- x resummation of differential distributions in our approach, we need to compute the coefficient function of the partonic subprocess where two off-shell gluons produce the final state. At lowest order, as appropriate for LL resummation, the process is

$$g^*(k_1) + g^*(k_2) \rightarrow Q(p) + \bar{Q}(\bar{p}), \tag{3.2}$$

where the off-shell gluon momenta are parametrized as⁸

$$k_1 = x_1 P_1 + \mathbf{k}_1, \tag{3.3a}$$

$$k_2 = x_2 P_2 + \mathbf{k}_2. \tag{3.3b}$$

In this way, the off-shellness of the gluons is given by a transverse component with respect to the beam axis. The longitudinal momentum fractions $x_{1,2}$ correspond to the first argument of the unintegrated PDFs, and their ratio is related to the longitudinal boost of the partonic reference frame used to compute the coefficient function by $Y - \eta = \frac{1}{2} \log \frac{x_1}{x_2}$. Note that this frame is not in general the partonic center-of-mass frame due to the presence of a transverse component in the gluon momenta, but it reduces to it in the limit where the gluons are on shell. Additional information on the kinematics is given in Appendix A.

In order to compute the actual off-shell coefficient function, we need to decide which is the vector q with respect

to which we want to be differential. There are two natural choices: either q is one of the two heavy quark momenta p or \bar{p} , or it is the sum of the two momenta, thus representing the momentum of the pair. We now present results for either choice in turn.

3.1 Results differential in the single heavy-quark

In this section we consider the final state to be one of the heavy quarks, and thus focus on the differential distribution in the components of the momentum $q = p$. The details of the computation of the partonic off-shell coefficient function are given in Appendix A.1.

We start by presenting the resummed result at parton level, computed according to Eqs. (2.33). We consider the resummed coefficient functions for bottom pair production, with $m_b = 4.6$ GeV, double differential in (partonic) rapidity y and transverse momentum p_t of the bottom quark.⁹ In Fig. 1, we show such distribution as a function of y and for fixed $p_t = 2$ GeV, which is a value accessible at LHCb for the production of b -hadrons. In the left panel, we plot separately the regular Eq. (2.34) and auxiliary Eq. (2.35) contributions out of which the various channels can be built according to Eqs. (2.33), while, in the right panel, we combine them according to those equations to construct the coefficient functions for the gg, gq, qg and qq channels. We observe that the shapes of these functions are quite peculiar, mostly due to the peak of the auxiliary contribution at large rapidity. However, we stress that these are parton-level results, and they are not expected to behave smoothly. In fact, due to the all-order nature of these contributions, it is natural that they present some new features missing in the fixed order.

To appreciate the effect of the resummed contributions on physical cross sections, we present the differential distributions after convolution with the PDFs in Fig. 2, considering for definiteness bottom pair production at LHC 13 TeV. We use the NNPDF31sx [23] PDF set that has been obtained in the context of a study on the inclusion of small- x resummation in PDF fits. The advantage of this set is that it provides PDFs consistently obtained with and without the inclusion of small- x resummation. In the following, we will use the same fixed-order PDFs to compute both the fixed-order and the resummed result, in order to emphasise the effect of resummation in the perturbative coefficient. Also, we provide resummed results obtained with the resummed PDFs, to see how much the resummation in PDFs impacts the cross section. However, performing a thorough phenomenological study is beyond the scope of this paper and is left to future work.

⁷ This simplification does not raise concerns about infrared safety, as the mass of the heavy quarks acts as an infrared regulator for the final state.

⁸ Here we are using a slightly inconsistent notation. Indeed, we assume that the bold vectors $\mathbf{k}_{1,2}$ are 2-dimensional Euclidean vectors in the transverse plane. However, when they are summed to 4-dimensional Minkowski vectors, we mean them to be the 4-vector with the same spatial components. The confusion may only arise when they appear in a scalar product, because the two interpretations would differ by a sign. In these cases, we always consider them as 2-vectors.

⁹ As we consider the bottom quarks to be on shell, the invariant mass distribution is a delta function and therefore for this process the triple differential distribution is of no interest.

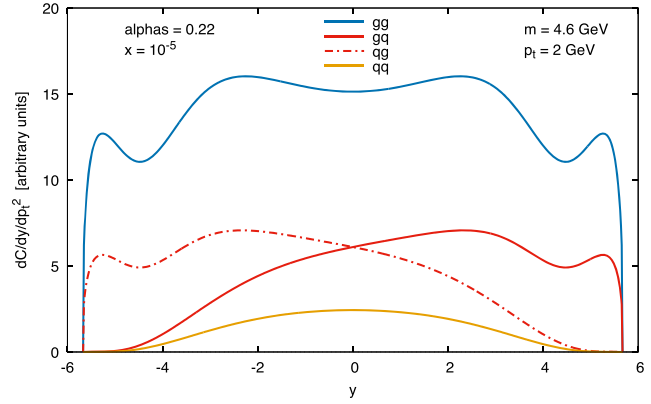
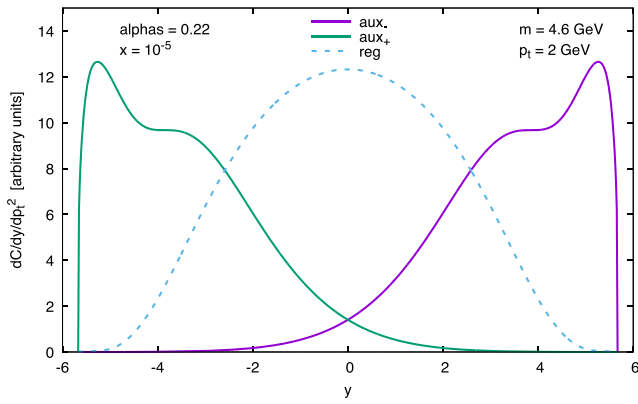


Fig. 1 The auxiliary Eq. (2.35) and regular Eq. (2.34) functions as a function of partonic rapidity y for single quark production of mass $m = 4.6$ GeV at $p_t = 2$ GeV and $x = 10^{-5}$ (left plot). The resummed

coefficient functions at parton level for each partonic channel constructed according to Eq. (2.33) for the same kinematics (right plot)

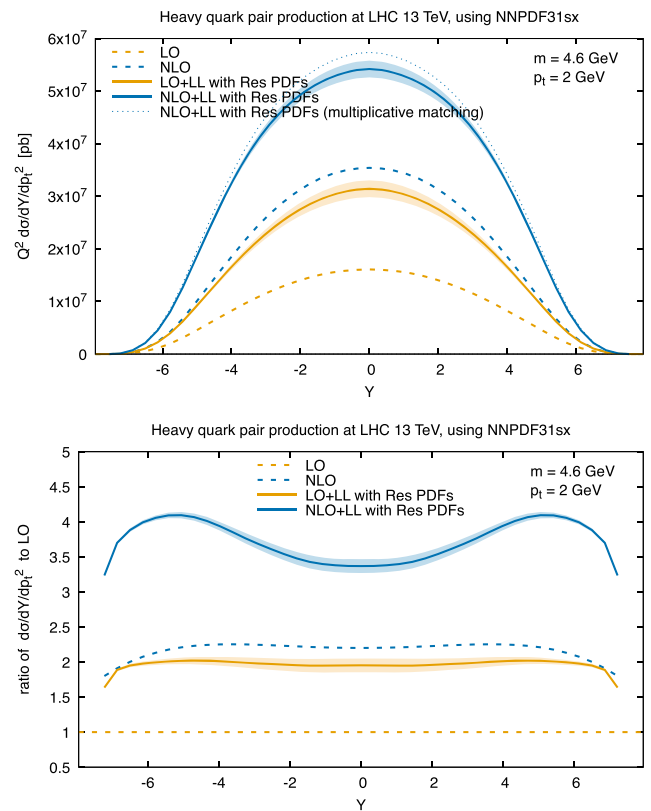
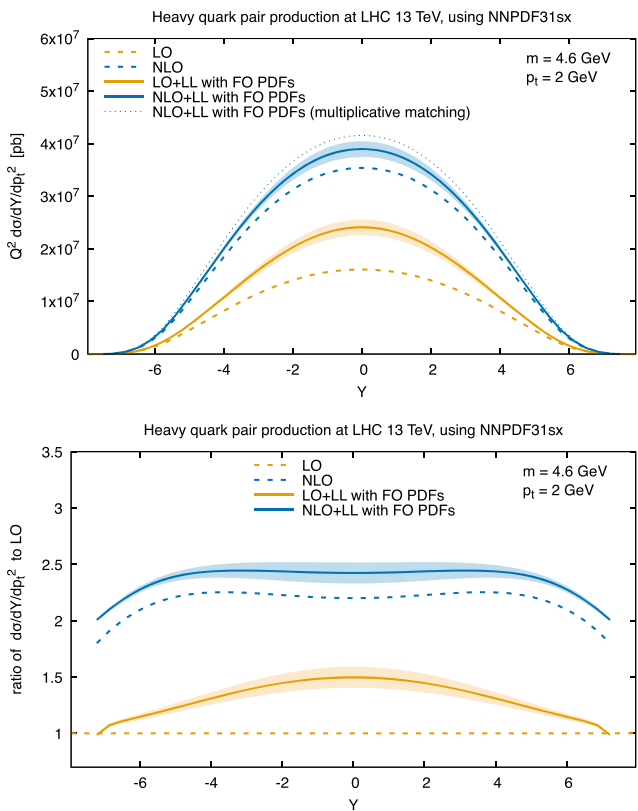


Fig. 2 The double differential distribution in rapidity and transverse momentum of the bottom quark, plotted as a function of the rapidity for $p_t = 2$ GeV, for bottom pair production at LHC 13 TeV. The left plots are obtained using NNPDF31sx at fixed order, while in the right

plot the resummed result is computed with the resummed PDFs from the same family. The uncertainty band represents an estimate of NLL corrections

The plots of Fig. 2 show the double differential distribution in rapidity Y and transverse momentum p_t at various orders (upper plots) and their ratio to the LO (lower plots), as a function of Y and for fixed $p_t = 2$ GeV. In the left plots, we use the same (fixed-order) PDFs for both fixed-

order results and resummed results. We show the LO cross section in dashed orange and the NLO one in dashed blue. The latter, obtained from POWHEG-box [56–58], is about twice as large as the LO result, which is partly due to the large value

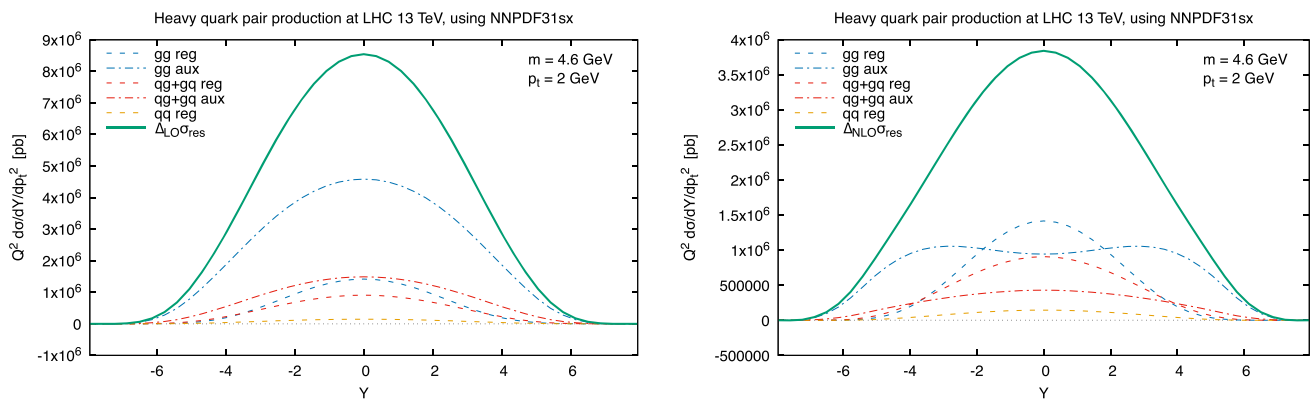


Fig. 3 Breakdown of the individual contributions to the resummed result from the gg , $gq + qg$ and qq channels separating the regular and auxiliary parts. The left plot focuses on the resummed contribution to be

matched to the LO, while the right plot focuses on the resummed contribution to be matched to NLO. The results in these plots are obtained using NNPDF31sx with resummation

of α_s at this low scale.¹⁰ In solid we plot the LO+LL (orange) and NLO+LL (blue) results. We observe that resummation is a positive correction at LO, of about 50% at central rapidity and decreasing towards the rapidity endpoints. At NLO, the correction of resummation is still positive, but smaller in size, showing that the perturbative expansion converges better when resummation is included. Overall, the NLO+LL result is approximately a 140% correction over the LO across the whole rapidity range except towards the endpoints, where it goes down a bit following the analogous behaviour of the NLO. When the resummed LO+LL and NLO+LL results are computed with resummed PDFs (right plots), the impact of resummation becomes much larger, as a consequence of the fact that the resummed gluon is larger than the fixed-order one at small x [23–25]. In particular, the NLO+LL curve has a large K-factor at large rapidities, where the contribution from the gluon at small x is dominant. This shows that this observable is very sensitive to the PDFs at small x , and it thus represents an important process to give additional constraints to PDF fits, in agreement with the findings of Refs. [59–61].

It is interesting to understand how the various contributions add up to form the resummed result. First of all, we stress that the LO cross section is made of two contributions, one in the gg channel and one in the $q\bar{q}$ channel. The second one, however, is very small, so the LO curve is almost entirely given by its gg contribution. As far as the resummed result is concerned, we not only distinguish between channels but also between the regular and auxiliary contributions, as given in Eqs. (2.33). The breakdown of the individual resummed contributions to be added to the LO is shown in Fig. 3 (left). We observe that the dominant contributions are those com-

ing from the auxiliary part, both in the gg channel and in the $gq + qg$ channel. The regular contributions are smaller and localised in a region of central rapidity. Also, we note a clear hierarchy in the contributions by the various channels, with the gg dominating over the $gq + qg$, and the qq being very small. We also stress that the $gq + qg$ channel is symmetric because we plot them together, but each individual contribution, qg and gq , is obviously asymmetric (see Fig. 1). The right plot of Fig. 3 shows the analogous breakdown for the resummed contribution to be added to the NLO to construct the NLO+LL result. The difference here is only in the auxiliary contributions, as the regular contribution starts at relative $\mathcal{O}(\alpha_s^2)$ and is thus unaffected when subtracting the expansion at $\mathcal{O}(\alpha_s)$. Because of this subtraction, the auxiliary contributions become comparable with the regular ones at mid rapidities, but they still dominate in the forward region, as expected.

In order to understand the stability of the resummed result, we now discuss its uncertainties. Because our resummed results are accurate at LL only, the first uncertainty we consider is the one coming from the unknown subleading logarithmic contributions. In previous HELL works [29–31, 48] such uncertainty is studied by varying subleading ingredients in the construction of the resummed anomalous dimension entering the evolution function Eq. (2.19) in two different ways,¹¹ and by varying the form of the evolution function itself by replacing $r(N, \alpha_s)$, Eq. (2.21) with $\alpha_s \beta_0$. The effect of these three independent ways of varying subleading logarithms in the resummed result is then added in quadrature

¹⁰ We use $\mu_R = \mu_F = m_b$, which is not the standard choice in POWHEG and probably not the best choice in terms of stability of the perturbative expansion, but it allows a simple matching with the resummed contribution.

¹¹ One variation is given by a modified way of implementing the resummation of subleading running coupling contributions in the anomalous dimension [30]. The other variation makes use of what we called LL' anomalous dimension introduced in Ref. [29] in place of the full NLL one, which gives by far the largest contribution to the uncertainty (see also Ref. [31]).

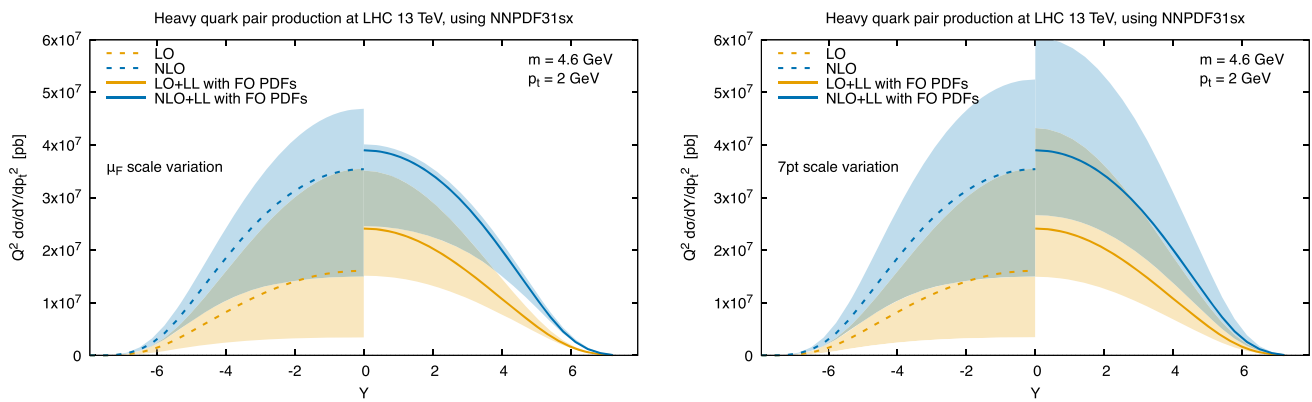


Fig. 4 Scale uncertainty for the double differential distribution in rapidity and transverse momentum of the bottom quark, plotted as a function of the rapidity for $p_t = 2$ GeV, for bottom pair production at

LHC 13 TeV. The left plot shows factorization scale uncertainty only, while the right plot shows the standard 7-point uncertainty envelope

to form a representative uncertainty for the final result. We adopt this procedure here, and we show the resulting uncertainty as a band in Fig. 2. While this way of computing the uncertainties may possibly underestimate the actual size of NLL contributions, it is clear from the plot that the difference between LO+LL and NLO+LL cannot be due to subleading logarithms only, as it is much larger than their uncertainty. Therefore, at this scale and value of p_t , contributions that are subleading power at small x are important. This can be seen also by looking at the difference between additive matching (our default) and multiplicative matching,¹² shown as a dotted line in the plot. The difference between these two curves, being related to the ratio between the exact NLO and its small- x approximation, also includes the effect of subleading power contributions, and it is indeed outside the uncertainty band from subleading logarithms.

In Fig. 4 we also show the scale uncertainty band of our results. In the left plot, we consider only the factorization scale variation by a canonical factor of 2 up and down, while in the right plot we construct the envelope of the customary 7-point variation of μ_F and μ_R . Because the rapidity distribution is symmetric, in each plot we show the fixed-order result for negative rapidity and the resummed result for positive rapidity, for a better visualisation of the bands. As far as μ_F variation is concerned, we note a clear reduction of the uncertainty after the inclusion of the resummation, demonstrating the perturbative stabilisation that small- x resummation allows to achieve. However, the uncertainty of the resummed result becomes comparable to the one of the fixed order once μ_R

variations are also taken into account. This is not surprising, for two reasons. The first one is that the value of α_s varies significantly as μ_R changes because the scale of the process is low (for the same reason, the NLO uncertainty is larger than the LO one). The other reason is that at LL there are no logarithms of μ_R in the resummed result to compensate for the change in α_s , as μ_R dependence in the resummation starts at NLL. To see a reduction of the 7-point uncertainty band the resummation should be performed at the currently unknown NLL order.

To conclude the section, we now consider the same double differential rapidity distribution but as a function of p_t at fixed central rapidity $Y = 0$. This is shown with fixed-order PDFs in Fig. 5. We observe that going towards large transverse momentum two effects are manifest: the NLO correction grows, and the impact of resummation on the LO gets larger while matching resummation to NLO gives a smaller correction. This suggests that the large NLO contribution at large p_t is dominated by small- x logarithms, and once these are resummed the perturbative convergence improves significantly. As the resummation has no direct dependence on the transverse momentum other than in kinematic constraints, this is just a consequence of the kinematics. In particular, we suspect that the smaller available phase space at large p_t makes contributions from the low- x region dominant also at central rapidity (at large rapidity this is expected at any p_t). We plan to investigate this effect further in future phenomenological studies.

3.2 Results differential in the heavy-quark pair

In this section we consider the final state to be the heavy-quark pair, and so focus on the differential distribution in the components of the momentum $q = p + \bar{p}$ which is the sum of the momenta of the two heavy quarks. For instance, this

¹² We recall that additive matching means that the resummed contribution is added to the fixed order subtracting the doubly counted contributions (corresponding to the expansion of the resummed result up to the order at which the fixed order is computed), while in the multiplicative matching the fixed order is multiplied by the resummed result divided by its expansion.

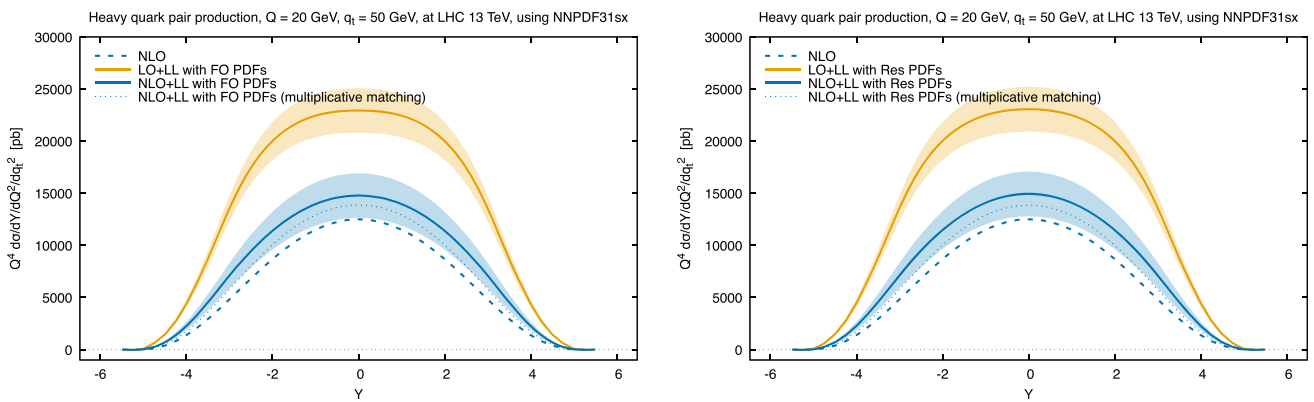


Fig. 6 The triple differential distribution in invariant mass, rapidity and transverse momentum of the bottom pair, plotted as a function of the rapidity for $Q = 20$ GeV and $p_t = 50$ GeV, for bottom pair production at LHC 13 TeV. The left plots are obtained using NNPDF31sx

at fixed order, while in the right plot the resummed result is computed with the resummed PDFs from the same family. The uncertainty band represents an estimate for the NLL corrections

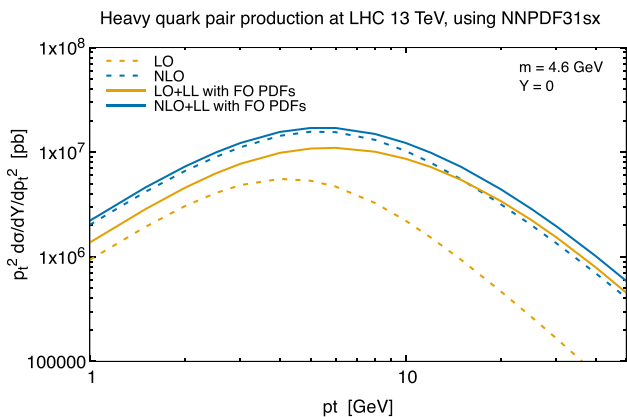


Fig. 5 The double differential distribution in rapidity and transverse momentum of the bottom quark, plotted as a function of p_t for central rapidity $Y = 0$, for bottom pair production at LHC 13 TeV

choice is appropriate for describing the measurement of a bound state of the heavy quarks, e.g. the J/ψ for $c\bar{c}$ pairs or the Υ for $b\bar{b}$ pairs or heavier resonances. The details of the computation of the partonic off-shell coefficient function are given in Appendix A.2. Because at the lowest order the process is effectively a 2 to 1 process, the differential coefficient function contains delta functions, Eq. (A.48). This implies that the computation of some of the integrals defining the resummed collinear coefficient functions, as described in Sect. 2.3, can be carried out analytically, partly simplifying the numerical implementation. Explicit expressions are presented in Appendix B.

Note that these simplifications pose some problems in presenting the results. Indeed, for instance, for the triple differential distribution the regular coefficient function Eq. (2.34) is an actual function, while the auxiliary coefficient Eq. (2.35) is a distribution, making a visual comparison at parton level

impossible. This problem can be overcome by showing the cross section at hadron level only, after integration with the PDFs. For definiteness, we consider bottom pair production at LHC 13 TeV, with bottom mass $m_b = 4.6$ GeV, as done in the previous section. Similarly, we use the same NNPDF31sx [23] PDF set considered before.

In Fig. 6 we show the triple differential distribution, plotted as a function of the rapidity Y of the pair and at fixed invariant mass $Q = 20$ GeV and fixed transverse momentum $q_t = 50$ GeV. In this case, the LO curve is not present, as it is proportional to $\delta(q_t^2)$, and so it is zero for any non-zero value of the transverse momentum. Consequently, we cannot show a ratio plot. We observe that the NLO (blue dashed curve) is smaller than the LL curve (solid orange), which is effectively a LO+LL result. After matching with the NLO, the resummed NLO+LL curve (solid blue) represents a small positive correction to the NLO result, pointing toward the still larger LL prediction. This suggests that the inclusion of resummation tends to predict a higher cross section than at NLO, and possibly leads to a better convergence of the perturbative expansion. As we did for Fig. 2, we show on the left the resummed result computed with the same fixed-order PDFs used for the NLO, while we show on the right panel the resummed contribution computed using the resummed PDFs. In this case, the difference between the two options is very mild, probably due to the larger value of τ and the larger invariant mass, showing that this observable is not particularly powerful in constraining the PDFs at small x .

Similarly to Fig. 3, we also show the breakdown of the individual contributions to the cross section in Fig. 7. When matching to LO (left plots) we note a pattern similar to what was observed for the single-quark distributions in the previous section. Namely, the auxiliary term dominates over the regular contribution, and the gg channel is larger than the

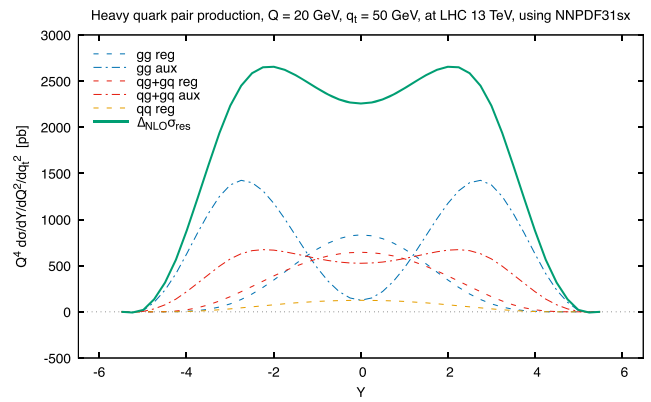
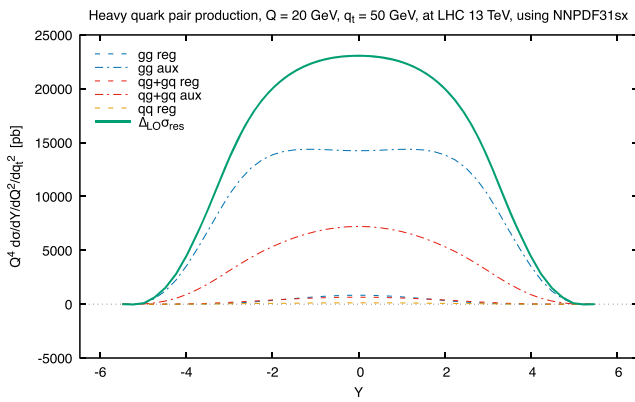


Fig. 7 Breakdown of the individual contributions to the resummed triple differential distribution in invariant mass, rapidity and transverse momentum of the bottom pair from the gg , $gq + qg$ and qq channels separating the regular and auxiliary parts. The left plot focuses on the resummed contribution to be matched to the LO, while the right

plot focuses on the resummed contribution to be matched to NLO. The results in these plots are obtained using NNPDF31sx with resummation at LHC 13 TeV, as a function of the rapidity, for invariant mass $Q = 20$ GeV and for transverse momentum $q_t = 50$ GeV

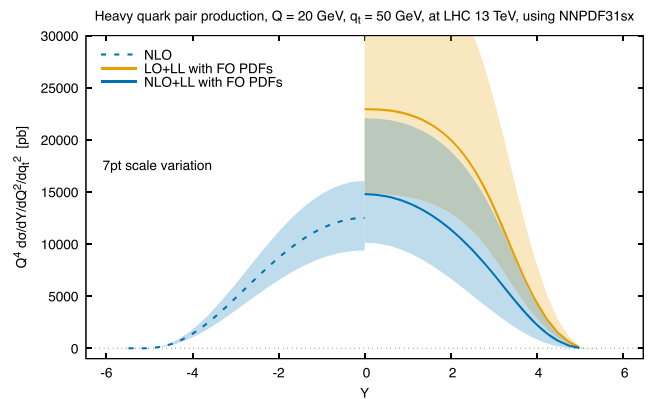
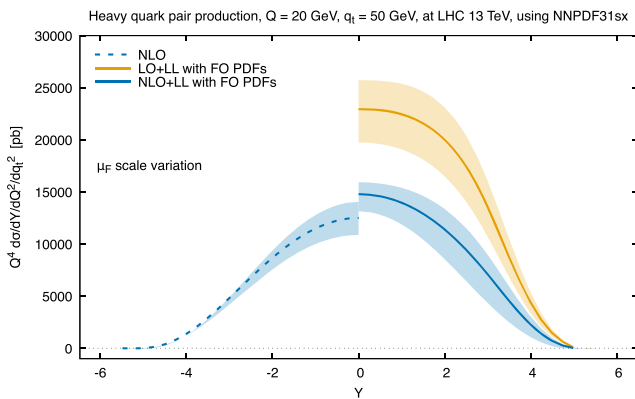


Fig. 8 Scale uncertainty for the triple differential distribution in rapidity and transverse momentum of the bottom quark pair, plotted as a function of the rapidity for $p_t = 50$ GeV, for bottom pair production at

LHC 13 TeV. The left plot shows factorization scale uncertainty only, while the right plot shows the standard 7-point uncertainty envelope

$qg + gq$, in turn larger than the qq channel. The resummed contribution is positive, consistent with the fact that this pure LL distribution is effectively a LO+LL result. When subtracting the $\mathcal{O}(\alpha_s)$ expansion to match the resummation to NLO (right plots) we find a smaller contribution from resummation. Again, we note that the auxiliary contributions are now comparable in size with the regular ones at mid rapidities, but they keep giving a much larger contribution at large rapidities.

We conclude the section by briefly commenting on the uncertainties. In Fig. 6 the resummed curves are supplemented with an uncertainty band computed as discussed in the previous section to estimate the impact of subleading logarithmic contributions. This uncertainty is relatively larger than in the case of single-quark kinematics, but still it cannot account for the full difference between LO+LL and NLO+LL, which thus gets significant contributions from

non-small- x effects. The use of multiplicative matching at NLO+LL, probing some subleading power contributions, differs from the additive matching by an amount that is comparable with the uncertainty band from subleading logarithms. Moving to scale variations, we show in Fig. 8 μ_F variations on the left plot and a full 7-point variation on the right plot. Considerations similar to what we have done for the single-quark kinematics apply. We limit ourselves to observe that in both plots there is a visible reduction moving from LO+LL to NLO+LL, again hinting at a stabilisation of the perturbative expansion once resummation is included.

Further studies of different distributions and different kinematic configurations, relevant for phenomenological applications, are beyond the scope of this more theoretical paper and are left to future work.

4 Conclusions

In this paper we have extended the HELL formalism for the small- x resummation of physical observables to differential distributions at LL. We have obtained resummed formulae for differential partonic coefficient functions which are valid for any process that is gluon–gluon initiated at LO. The application of the formalism to other kinds of processes requires the treatment of collinear subtractions to all orders at small x , whose extension at differential level is left to future work [39].

With respect to previous implementations of small- x resummation, we no longer perform an approximation, valid at LL, where the off-shell coefficient function was computed at $N = 0$ in Mellin space. This approximation simplifies the resummation of inclusive cross sections where such Mellin transform could be computed analytically. Here, because in general we are not able to compute this Mellin transform analytically at differential level, adopting such approximation would not lead to any simplification. Rather, it would break the kinematic limits of the observables, which is clearly undesirable.

We have considered heavy-quark pair production at proton–proton colliders as a representative application of our results. We have resummed distributions differential both in the momentum of a single heavy quark and in the sum of the momenta of both heavy quarks (momentum of the pair). The selection of numerical results presented serves as a demonstration that the methodology works and that it can be used for phenomenology. They also show that the impact of small- x resummation for these observables is significant, as we expect from the low- x values that heavy quark pair production can reach at LHC. However, the results presented in this work do not represent a full phenomenological study, that would also require the description of the hadronisation of the heavy quarks in order to compare with the data. Such a phenomenological study, with the goal to include the process in a PDF fit to improve the PDF quality at low x , is left to future work.

The new version of the HELL code, that implements the resummation of heavy quark pair production at differential level, is available at the url

www.roma1.infn.it/~bonvini/hell

The preparation of tables for quick interpolation, needed for phenomenological applications, requires some time and leads to a large amount of data, because of the dependence on many kinematic variables. Therefore, rather than providing general tables within the code (as previously done for DIS and Higgs), we only provide scripts for the generation of such tables, which can then be produced and used directly by the user focussing only on the kinematics of interest.

Acknowledgements We thank Simone Marzani, Luca Rottoli and Francesco Giovanni Celiberto for several useful discussions and for comments on the manuscript. The work of MB was supported by the Marie Skłodowska Curie grant HiPPiE@LHC under the agreement n. 746159.

Data Availability Statement This manuscript has no associated data or the data will not be deposited. [Authors' comment: No data is associated to this work due to its theoretical nature.]

Open Access This article is licensed under a Creative Commons Attribution 4.0 International License, which permits use, sharing, adaptation, distribution and reproduction in any medium or format, as long as you give appropriate credit to the original author(s) and the source, provide a link to the Creative Commons licence, and indicate if changes were made. The images or other third party material in this article are included in the article's Creative Commons licence, unless indicated otherwise in a credit line to the material. If material is not included in the article's Creative Commons licence and your intended use is not permitted by statutory regulation or exceeds the permitted use, you will need to obtain permission directly from the copyright holder. To view a copy of this licence, visit <http://creativecommons.org/licenses/by/4.0/>.

Funded by SCOAP³. SCOAP³ supports the goals of the International Year of Basic Sciences for Sustainable Development.

Appendix A: The off-shell coefficient function

In this Appendix we give all the details for the computation of the off-shell coefficient function for heavy quark pair production at proton–proton colliders. The partonic process at the lowest order, relevant for LL resummation, is

$$g^*(k_1) + g^*(k_2) \rightarrow Q(p) + \bar{Q}(\bar{p}). \quad (\text{A.1})$$

where Q and \bar{Q} are the two heavy quarks of mass m . We parametrize the momenta as

$$k_1 = x_1 P_1 + \mathbf{k}_1 \quad (\text{A.2a})$$

$$k_2 = x_2 P_2 + \mathbf{k}_2 \quad (\text{A.2b})$$

$$p = z_1 x_1 P_1 + z_2 x_2 P_2 + \mathbf{p} \quad (\text{A.2c})$$

$$\bar{p} = (1 - z_1)x_1 P_1 + (1 - z_2)x_2 P_2 + \mathbf{k}_1 + \mathbf{k}_2 - \mathbf{p}, \quad (\text{A.2d})$$

where, in the collider center-of-mass frame, the protons momenta are

$$P_1 = \frac{\sqrt{s}}{2}(1, 0, 0, 1), \quad P_2 = \frac{\sqrt{s}}{2}(1, 0, 0, -1). \quad (\text{A.3})$$

In these definitions we have already used momentum conservation, and we have made a choice of reference frame. There are 7 initial-state parameters ($s, x_1, x_2, \mathbf{k}_1, \mathbf{k}_2$) and 4 final-state parameters (z_1, z_2, \mathbf{p}). Note however that using the on-shell condition for the final-state quarks we can constrain one of the final-state parameters. Indeed, there are two on-shell conditions,

$$m^2 = p^2 = z_1 z_2 x_1 x_2 s - |\mathbf{p}|^2 \quad (\text{A.4a})$$

$$m^2 = \bar{p}^2 = (1 - z_1)(1 - z_2)x_1x_2s - |\mathbf{k}_1 + \mathbf{k}_2 - \mathbf{p}|^2, \tag{A.4b}$$

setting the squared momenta p^2 and \bar{p}^2 to the *same* mass m^2 . Therefore, only three of the four final state parameters are independent.

The partonic off-shell coefficient function is computed in the ‘‘partonic’’ reference frame, that corresponds to the partonic center-of-mass frame if the two gluons were on shell, namely if $\mathbf{k}_1 = \mathbf{k}_2 = 0$. In other words, the partonic frame is related to the collider frame by a longitudinal boost of rapidity

$$\bar{\eta} = \frac{1}{2} \log \frac{x_1}{x_2}. \tag{A.5}$$

In this frame, the partonic coefficient can only depend on x_1, x_2 and s through the product x_1x_2s . Moreover, because we assume unpolarized protons, an overall azimuthal angle is irrelevant. Thus the coefficient can only depend on 4 out of the 7 initial-state parameters. We choose them to be

$$z \equiv \frac{Q^2}{x_1x_2s} \tag{A.6a}$$

$$\xi_1 \equiv \frac{|\mathbf{k}_1|^2}{Q^2} \tag{A.6b}$$

$$\xi_2 \equiv \frac{|\mathbf{k}_2|^2}{Q^2} \tag{A.6c}$$

$$\varphi \equiv \text{angle between } \mathbf{k}_1 \text{ and } \mathbf{k}_2. \tag{A.6d}$$

Here, Q^2 is ‘‘the hard scale’’, whose value depends on the final state we want to look at. We set $Q^2 = q^2$, where q is the final state momentum with respect to which we want to be differential. In particular, if we want to study the kinematics of the heavy-quark pair, then $q = p + \bar{p}$ and Q^2 is the squared invariant mass of the pair, while for the single heavy quark then $q = p$ and $Q^2 = m^2$ is the mass squared of the quark itself.

Before discussing each of these cases in turn, we note that x_1x_2s is *not* $\hat{s} = (k_1 + k_2)^2 = x_1x_2s - |\mathbf{k}_1 + \mathbf{k}_2|^2$, because of the transverse component of the gluons; we may call it the ‘‘longitudinal part’’ of \hat{s} (meaning the contribution to \hat{s} due to the longitudinal part of the gluon momenta). The full partonic center-of-mass energy \hat{s} can be written as

$$\hat{s} = Q^2 \left[\frac{1}{z} - \xi_1 - \xi_2 - 2\sqrt{\xi_1\xi_2} \cos \varphi \right] \tag{A.7}$$

in terms of the new variables, which reduces to the usual expression $\hat{s} = Q^2/z$ when the gluons are on shell.

A.1 Kinematics for the single quark

Here we consider the differential distribution in the kinematics of one of the final-state heavy quarks. For definiteness, we consider the heavy quark of momentum p , but since the process is symmetric the results will equally apply also to the antiquark with momentum \bar{p} . We introduce the variables

$$Q^2 \equiv p^2 = z_1z_2x_1x_2s - |\mathbf{p}|^2 = m^2 \tag{A.8a}$$

$$\eta \equiv \frac{1}{2} \log \frac{p^0 + p^3}{p^0 - p^3} - \bar{\eta} = \frac{1}{2} \log \frac{z_1}{z_2} \tag{A.8b}$$

$$\hat{p}_t^2 \equiv \frac{\mathbf{p}^2}{Q^2} = \frac{\mathbf{p}^2}{m^2} \tag{A.8c}$$

$$\vartheta = \text{angle between } \mathbf{p} \text{ and } \mathbf{k}_1 + \mathbf{k}_2. \tag{A.8d}$$

Because $Q^2 = m^2$ is fixed, the most differential distribution we are interested in is $(p_t^2 = \hat{p}_t^2 Q^2)$

$$\frac{dC}{d\eta dp_t^2}(z, \xi_1, \xi_2, m^2, \eta, \hat{p}_t^2), \tag{A.9}$$

which is integrated over ϑ and averaged over φ . Note that from now on we are omitting the argument α_s from the off-shell distribution as we are interested in the lowest order result only.

Let us consider the phase space. The two-body phase space is given by

$$\begin{aligned} d\phi_2(k_1 + k_2; p, \bar{p}) &= \theta(\hat{s} - 4m^2) \frac{d^4p}{(2\pi)^3} \frac{d^4\bar{p}}{(2\pi)^3} \delta(p^2 - m^2) \delta(\bar{p}^2 - m^2) \\ &\quad \times (2\pi)^4 \delta^{(4)}(k_1 + k_2 - p - \bar{p}) \theta(p^0) \theta(\bar{p}^0) \\ &= \theta(\hat{s} - 4m^2) \frac{d^4p}{4\pi^2} \delta(p^2 - m^2) \delta((k_1 + k_2 - p)^2 - m^2) \\ &\quad \times \theta(p^0) \theta(k_1^0 + k_2^0 - p^0) \end{aligned} \tag{A.10}$$

with $\hat{s} = (k_1 + k_2)^2$. We need to express this phase space in terms of the new variables. The variable \hat{s} is given in Eq. (A.7), the integration element can be written as

$$d^4p = \frac{Q^2}{4} dQ^2 d\eta d\hat{p}_t^2 d\vartheta, \tag{A.11}$$

and the antiquark momentum squared is

$$\begin{aligned} \bar{p}^2 &= (k_1 + k_2 - p)^2 \\ &= (1 - z_1)(1 - z_2)x_1x_2s - |\mathbf{k}_1 + \mathbf{k}_2 - \mathbf{p}|^2 \\ &= Q^2 \left[1 + \frac{1}{z} - \sqrt{\frac{1 + \hat{p}_t^2}{z}} (e^\eta + e^{-\eta}) - \xi_1 - \xi_2 \right. \\ &\quad \left. - 2\sqrt{\xi_1\xi_2} \cos \varphi \right] \end{aligned}$$

$$+ 2\sqrt{(\xi_1 + \xi_2 + 2\sqrt{\xi_1\xi_2} \cos \varphi)} \hat{p}_t^2 \cos \vartheta \Big], \tag{A.12}$$

where we have used the inverse relations

$$z_1 = \sqrt{z(1 + \hat{p}_t^2)} e^\eta, \quad z_2 = \sqrt{z(1 + \hat{p}_t^2)} e^{-\eta}. \tag{A.13}$$

To simplify the notation, we introduce the function

$$\xi(\xi_1, \xi_2, \varphi) = \xi_1 + \xi_2 + 2\sqrt{\xi_1\xi_2} \cos \varphi = |\mathbf{k}_1 + \mathbf{k}_2|^2, \tag{A.16}$$

and simply write ξ without arguments for short. Putting everything together we have

$$\begin{aligned} \frac{Q^2 d\mathcal{C}}{d\eta d p_t^2}(z, \xi_1, \xi_2, m^2, \eta, \hat{p}_t^2) &= \sigma_0 \frac{1}{2} \int_0^{2\pi} \frac{d\varphi}{2\pi} \int \frac{d\phi_2}{d\eta d\hat{p}_t^2} |\mathcal{M}|^2 = \frac{\sigma_0}{32\pi^2} \int_0^{2\pi} \frac{d\varphi}{2\pi} \theta\left(\frac{1}{z} - \xi - 4\right) \theta\left(\frac{1}{z} - (1 + \hat{p}_t^2)e^{2|\eta|}\right) \\ &\times \int_0^{2\pi} d\vartheta |\mathcal{M}|^2 \delta\left(\frac{1}{z} - \sqrt{\frac{1 + \hat{p}_t^2}{z}}(e^\eta + e^{-\eta}) - \xi + 2\sqrt{\xi \hat{p}_t^2} \cos \vartheta\right), \end{aligned} \tag{A.17}$$

The conditions imposed by the two theta functions in the energies translate easily into conditions on z_1 and z_2 that depend on x_1 and x_2 , namely $z_1 x_1 + z_2 x_2 \geq 0$ and $(1 - z_1)x_1 + (1 - z_2)x_2 \geq 0$. From the on-shell conditions Eq. (A.4) we also know that $z_1 z_2 x_1 x_2 \geq 0$ and $(1 - z_1)(1 - z_2)x_1 x_2 \geq 0$. Because x_1 and x_2 are positive, it follows that z_1 and z_2 satisfy the conditions $0 \leq z_{1,2} \leq 1$, that translate into

$$z(1 + \hat{p}_t^2) \leq e^{-2|\eta|}. \tag{A.14}$$

After the trivial integration over Q^2 , the phase space can thus be recast as

where in the first line $1/2$ is the flux factor, $\sigma_0 = 16\pi^2 \alpha_s^2 / Q^2$ and the $1/2\pi$ comes from the average over φ . The matrix element squared $|\mathcal{M}|^2$ is given in Appendix A.3.

It is most convenient to use the δ function to integrate over ϑ , as all other variables appear at least quadratically. The fact that $|\cos \vartheta| \leq 1$ produces the constraint

$$\left| \frac{1}{z} - \sqrt{\frac{1 + \hat{p}_t^2}{z}}(e^\eta + e^{-\eta}) - \xi \right| \leq 2\sqrt{\xi \hat{p}_t^2}. \tag{A.18}$$

We then get

$$\begin{aligned} \frac{Q^2 d\mathcal{C}}{d\eta d p_t^2}(z, \xi_1, \xi_2, m^2, \eta, \hat{p}_t^2) &= \frac{\sigma_0}{32\pi^2} \int_0^{2\pi} \frac{d\varphi}{2\pi} \theta\left(\frac{1}{z} - \xi - 4\right) \theta\left(\frac{1}{z} - (1 + \hat{p}_t^2)e^{2|\eta|}\right) \\ &\times \theta\left(2\sqrt{\xi \hat{p}_t^2} - \left|\frac{1}{z} - \sqrt{\frac{1 + \hat{p}_t^2}{z}}(e^\eta + e^{-\eta}) - \xi\right|\right) \frac{|\mathcal{M}|_{\vartheta=\bar{\vartheta}}^2 + |\mathcal{M}|_{\vartheta=2\pi-\bar{\vartheta}}^2}{\sqrt{4\xi \hat{p}_t^2 - \left(\frac{1}{z} - \sqrt{\frac{1 + \hat{p}_t^2}{z}}(e^\eta + e^{-\eta}) - \xi\right)^2}}, \end{aligned} \tag{A.19}$$

$$\bar{\vartheta} = \cos^{-1} \frac{\xi - \frac{1}{z} + \sqrt{\frac{1 + \hat{p}_t^2}{z}}(e^\eta + e^{-\eta})}{2\sqrt{\xi \hat{p}_t^2}}, \quad 0 \leq \vartheta \leq \pi. \tag{A.20}$$

$$\begin{aligned} d\phi_2 &= \theta\left(\frac{1}{z} - \xi_1 - \xi_2 - 2\sqrt{\xi_1\xi_2} \cos \varphi - 4\right) \\ &\times \theta\left(\frac{1}{z} - (1 + \hat{p}_t^2)e^{2|\eta|}\right) \frac{1}{16\pi^2} d\eta d\hat{p}_t^2 d\vartheta \\ &\times \delta\left(\frac{1}{z} - \sqrt{\frac{1 + \hat{p}_t^2}{z}}(e^\eta + e^{-\eta}) - \xi_1 - \xi_2 \right. \\ &\quad \left. - 2\sqrt{\xi_1\xi_2} \cos \varphi \right. \\ &\quad \left. + 2\sqrt{(\xi_1 + \xi_2 + 2\sqrt{\xi_1\xi_2} \cos \varphi)} \hat{p}_t^2 \cos \vartheta\right). \end{aligned} \tag{A.15}$$

The theta functions in Eq. (A.19) may prove troublesome from a numerical point of view. Indeed, if used as “if” conditions that set the integrand to zero when the theta functions are zero, the numerical integration may become inaccurate. It is much more convenient to translate them into integration limits of some variable. To do so, we define

$$X = \frac{1}{\sqrt{z}} \geq 1 \tag{A.21}$$

so that the constraint imposed by the three theta functions become

$$X \geq \sqrt{4 + \xi}, \tag{A.22a}$$

$$X \geq \sqrt{1 + \hat{p}_t^2} e^{|\eta|}, \tag{A.22b}$$

$$-2\sqrt{\xi} \hat{p}_t \leq -X^2 + 2BX + \xi \leq 2\sqrt{\xi} \hat{p}_t, \tag{A.22c}$$

$$B \equiv \sqrt{1 + \hat{p}_t^2} \cosh \eta \geq 1.$$

Focussing on ξ , we may write

$$\xi \leq X^2 - 4, \tag{A.23a}$$

$$\xi + 2\hat{p}_t\sqrt{\xi} + 2BX - X^2 \geq 0, \tag{A.23b}$$

$$\xi - 2\hat{p}_t\sqrt{\xi} + 2BX - X^2 \leq 0. \tag{A.23c}$$

The functions $\xi \pm 2\hat{p}_t\sqrt{\xi} + 2BX - X^2$ represent two parabolas in $\sqrt{\xi}$ with centers (minima) in $\sqrt{\xi} = \mp \hat{p}_t$, at which they both equal $-\hat{p}_t^2 + 2BX - X^2$. If this value is positive, there is no solution to the system, so we have the condition

$$\hat{p}_t^2 - 2BX + X^2 \geq 0 \tag{A.24}$$

that represents an equation for the other variables to be taken into account later, together with Eq. (A.22b). Under this condition, the solution of the inequalities Eq. (A.23b), (A.23c) is the region between the two right solution of the second inequality and the largest between the right solution of the first and the left solution of the second, which are identical but have opposite sign. Thus we get

$$\left| \hat{p}_t - \sqrt{\hat{p}_t^2 - 2BX + X^2} \right| \leq \sqrt{\xi} \leq \hat{p}_t + \sqrt{\hat{p}_t^2 - 2BX + X^2}. \tag{A.25}$$

The other condition Eq. (A.23a) is always automatically satisfied. Indeed, we can prove that

$$\sqrt{X^2 - 4} \geq \hat{p}_t + \sqrt{\hat{p}_t^2 - 2BX + X^2} \tag{A.26}$$

for all meaningful values of X (namely values for which the square roots are real). Indeed this condition can be manipulated to

$$(B^2 - \hat{p}_t^2)X^2 - 4BX + 4(1 + \hat{p}_t^2) \geq 0, \tag{A.27}$$

which is always satisfied because the minimum of the quadratic function, located at $X = 2B/(B^2 - \hat{p}_t^2)$, is always non-negative. Indeed the minimum is proportional to $B^2 - 1 - \hat{p}_t^2$ which is non-negative because $B^2 \geq 1 + \hat{p}_t^2$. Therefore, Eq. (A.25) is the complete condition on ξ .

We now focus on the other variables, that must satisfy the inequalities Eq. (A.22b) and (A.24). Let us focus on Eq. (A.24), solving it for X . The parabola $X^2 - 2BX + \hat{p}_t^2$ has a minimum in $X = B$ where it equals $\hat{p}_t^2 - B^2$. This is always negative, as by construction $B^2 \geq 1 + \hat{p}_t^2 > \hat{p}_t^2$. Therefore, there are two separate solutions, $X \geq B + \sqrt{B^2 - \hat{p}_t^2}$ and

$X \leq B - \sqrt{B^2 - \hat{p}_t^2}$. However, since we always have

$$\sqrt{1 + \hat{p}_t^2} e^{|\eta|} \geq B, \tag{A.28}$$

the second solution is not compatible with Eq. (A.22b), and it is therefore forbidden. We are thus left with the condition

$$X \geq B + \sqrt{B^2 - \hat{p}_t^2} \geq B + 1 \geq 2, \tag{A.29}$$

together with Eq. (A.22b). We can show that Eq. (A.22b) is always compatible with Eq. (A.29). Indeed the inequality

$$B + \sqrt{B^2 - \hat{p}_t^2} \geq \sqrt{1 + \hat{p}_t^2} e^{|\eta|} \tag{A.30}$$

holds because we can manipulate it into

$$\sqrt{B^2 - \hat{p}_t^2} \geq \sqrt{1 + \hat{p}_t^2} (e^{|\eta|} - \cosh \eta) = \sqrt{1 + \hat{p}_t^2} \sinh |\eta| \tag{A.31}$$

and then, squaring both sides (which are both positive) and rearranging,

$$(1 + \hat{p}_t^2) (\cosh^2 |\eta| - \sinh^2 |\eta|) - \hat{p}_t^2 \geq 0 \Rightarrow 1 + \hat{p}_t^2 - \hat{p}_t^2 \geq 0 \tag{A.32}$$

which is clearly true. In conclusion, X satisfies only the inequality Eq. (A.29) which automatically encodes all the others.

It is useful to mention also the conditions on the kinematic limits of the on-shell resummed coefficient, as well as on the integration variables defining the resummed result. From Eq. (2.34), recalling that the first argument of the evolution function is a momentum fraction and is thus smaller than 1, we obtain the condition $x/z \leq e^{-2|\bar{\eta}|}$. Similarly, from Eq. (A.14) we also have $z(1 + \hat{p}_t^2) \leq e^{-2|\eta|}$. From the product of the two inequalities, we obtain the condition

$$A^2 \equiv x(1 + \hat{p}_t^2) \leq e^{-2|\eta| - 2|\bar{\eta}|} \leq e^{-2|\eta + \bar{\eta}|} = e^{-2|y|}. \tag{A.33}$$

The condition $A \leq e^{-|y|}$, with $A \equiv \sqrt{x(1 + \hat{p}_t^2)}$, represents a constraint on the arguments of the on-shell coefficient function. However, this is not the most stringent one. Indeed, looking at the first inequality, we can derive the integration range of $\bar{\eta}$, which is given by

$$\frac{Ae^y - x\hat{p}_t^2}{1 - Ae^{-y}} \leq e^{2\bar{\eta}} \leq \frac{1 - Ae^y}{Ae^{-y} - x\hat{p}_t^2}. \tag{A.34}$$

For this range to be non-trivial, the upper limit must be larger than the lower limit, leading to the condition

$$e^{|\eta|} \leq \frac{1 + x\hat{p}_t^2}{2A} + \sqrt{\frac{(1 + x\hat{p}_t^2)^2}{4A^2} - 1} \tag{A.35}$$

which is smaller than $1/\Lambda$ in the region where the square root exists, given by the condition $\hat{p}_t^2 \leq \frac{1-2\sqrt{x}}{x}$ or, equivalently,

$$x \leq \left(\frac{\sqrt{1 + \hat{p}_t^2} - 1}{\hat{p}_t^2} \right)^2 \leq \frac{1}{4}. \tag{A.36}$$

To conclude, we recall that the matrix element squared that we will present in Appendix A.3 must be expressed in terms of the variables defined here. To achieve this, we need to express z_1, z_2 in terms of \hat{p}_t, η through Eq. (A.13), and to write the product $\mathbf{k}_2 \cdot \mathbf{p}$ appearing in Eqs. (A.67c) and (A.67d) as

$$\frac{\mathbf{k}_2 \cdot \mathbf{p}}{Q^2} = \sqrt{\xi_2 \hat{p}_t^2} \cos(\vartheta + \varphi'), \tag{A.37}$$

where φ' is the angle of $\mathbf{k}_1 + \mathbf{k}_2$ with respect to \mathbf{k}_2 , which can be computed from the cartesian representation (aligning the x axis along \mathbf{k}_2)

$$\mathbf{q} = \begin{pmatrix} |\mathbf{q}| \cos \varphi' \\ |\mathbf{q}| \sin \varphi' \end{pmatrix} = \begin{pmatrix} |\mathbf{k}_2| + |\mathbf{k}_1| \cos \varphi \\ |\mathbf{k}_1| \sin \varphi \end{pmatrix} \tag{A.38}$$

leading to

$$\sin \varphi' = \frac{\sqrt{\xi_1} \sin \varphi}{\sqrt{\hat{q}_t^2}} \quad \cos \varphi' = \frac{\sqrt{\xi_2} + \sqrt{\xi_1} \cos \varphi}{\sqrt{\hat{q}_t^2}}, \tag{A.39}$$

which gives the result

$$\varphi' = \begin{cases} \cos^{-1} \left(\frac{\sqrt{\xi_2} + \sqrt{\xi_1} \cos \varphi}{\sqrt{\hat{q}_t^2}} \right) & \text{if } \sin \varphi \geq 0 \\ 2\pi - \cos^{-1} \left(\frac{\sqrt{\xi_2} + \sqrt{\xi_1} \cos \varphi}{\sqrt{\hat{q}_t^2}} \right) & \text{if } \sin \varphi < 0. \end{cases} \tag{A.40}$$

A.2 Kinematics for the pair

We now consider the heavy-quark pair as a fictitious intermediate state, with momentum

$$\begin{aligned} q &\equiv p + \bar{p} \\ &\equiv \alpha_1 x_1 P_1 + \alpha_2 x_2 P_2 + \mathbf{q} && \text{(generic parametrization)} \\ &= k_1 + k_2 && \text{(momentum conservation)} \\ &= x_1 P_1 + x_2 P_2 + \mathbf{k}_1 + \mathbf{k}_2, \end{aligned} \tag{A.41}$$

where by momentum conservation $\alpha_1 = \alpha_2 = 1$ and $\mathbf{q} = \mathbf{k}_1 + \mathbf{k}_2$. For this intermediate state, we introduce the variables¹³

$$\begin{aligned} Q^2 &\equiv q^2 = \alpha_1 \alpha_2 x_1 x_2 s - |\mathbf{q}|^2 = x_1 x_2 s - |\mathbf{k}_1 + \mathbf{k}_2|^2 \\ &= (k_1 + k_2)^2 \equiv \hat{s} \end{aligned} \tag{A.42a}$$

¹³ Note that we are using the same names Q^2 and η that we used for the single quark kinematics, now referring to another momentum.

$$\begin{aligned} \eta &\equiv \frac{1}{2} \log \frac{q^0 + q^3}{q^0 - q^3} - \bar{\eta} = \frac{1}{2} \log \frac{\alpha_1}{\alpha_2} = 0 \\ &\text{(rapidity of } q \text{ in the partonic frame)} \end{aligned} \tag{A.42b}$$

$$\hat{q}_t^2 \equiv \frac{\mathbf{q}^2}{Q^2} = \frac{|\mathbf{k}_1 + \mathbf{k}_2|^2}{Q^2} \tag{A.42c}$$

$$\psi \equiv \text{angle between } \mathbf{q} \text{ and } \mathbf{k}_1 + \mathbf{k}_2 = 0. \tag{A.42d}$$

Our goal is to compute the parton-level off-shell coefficient function ($q_t^2 = \hat{q}_t^2 Q^2$)

$$\frac{d\mathcal{C}}{dQ^2 d\eta dq_t^2}(z, \xi_1, \xi_2, Q^2, \eta, \hat{q}_t^2), \tag{A.43}$$

which is integrated over ψ and averaged over φ .

Let us consider the phase space. The two-body phase space of the two final state heavy quarks can be factorized into the phase space of the pair and its ‘‘decay’’ as

$$\begin{aligned} d\phi_2(k_1 + k_2; p, \bar{p}) &= \theta(\hat{s} - 4m^2) \\ &\times \int_{4m^2}^{\hat{s}} \frac{dq^2}{2\pi} d\phi_1(k_1 + k_2; q) d\phi_2(q; p, \bar{p}) \end{aligned} \tag{A.44}$$

where

$$\begin{aligned} d\phi_1(k_1 + k_2; q) &= \frac{d^4 q}{(2\pi)^3} \delta(q^2 - \hat{s}) (2\pi)^4 \delta^{(4)}(k_1 + k_2 - q) \\ &= 2\pi d^4 q \delta(q^2 - \hat{s}) \delta^{(4)}(k_1 + k_2 - q), \end{aligned} \tag{A.45}$$

with $\hat{s} = (k_1 + k_2)^2$ the invariant mass of the pair, and

$$\begin{aligned} d\phi_2(q; p, \bar{p}) &= \frac{d^4 p}{(2\pi)^3} \frac{d^4 \bar{p}}{(2\pi)^3} \delta(p^2 - m^2) \delta(\bar{p}^2 - m^2) \\ &(2\pi)^4 \delta^{(4)}(q - p - \bar{p}) \theta(p^0) \theta(\bar{p}^0). \end{aligned} \tag{A.46}$$

The full phase space Eq. (A.44) can be simplified using the delta function of the one-body phase space to perform the q^2 integral, giving

$$\begin{aligned} d\phi_2(k_1 + k_2; p, \bar{p}) &= \theta(\hat{s} - 4m^2) d^4 q \delta^{(4)}(k_1 + k_2 - q) d\phi_2(q; p, \bar{p}) \\ &= \theta(\hat{s} - 4m^2) dQ^2 d\eta d\hat{q}_t^2 d\psi d\phi_2(q; p, \bar{p}) \\ &\times \delta(Q^2 - \hat{s}) \\ &\delta(\eta) \delta(\hat{q}_t^2 - \xi_1 - \xi_2 - 2\sqrt{\xi_1 \xi_2} \cos \varphi) \delta(\psi) \\ &= \theta(Q^2 - 4m^2) dQ^2 d\eta d\hat{q}_t^2 d\psi d\phi_2(q; p, \bar{p}) \\ &\times \frac{1}{Q^2} \delta\left(1 + \hat{q}_t^2 - \frac{1}{z}\right) \delta(\eta) \\ &\times \delta(\hat{q}_t^2 - \xi_1 - \xi_2 - 2\sqrt{\xi_1 \xi_2} \cos \varphi) \delta(\psi), \end{aligned} \tag{A.47}$$

where we have rewritten d^4q , the delta function and \hat{s} in terms of the new variables.

The two-body phase space can be used to integrate the matrix element and remove the “internal” degrees of freedom of the pair, while the one-body phase space can be used to obtain the desired differential observable. Thus, we immediately find the relation

$$\begin{aligned} & \frac{Q^4 dC}{dQ^2 d\eta dq_t^2 d\varphi}(z, \xi_1, \xi_2, Q^2, \eta, \hat{q}_t^2, \varphi) \\ &= \frac{dC}{d\varphi}(z, \xi_1, \xi_2, Q^2, \varphi) \\ & \times \delta\left(1 + \hat{q}_t^2 - \frac{1}{z}\right) \delta(\eta) \\ & \times \delta\left(\hat{q}_t^2 - \xi_1 - \xi_2 - 2\sqrt{\xi_1 \xi_2} \cos \varphi\right), \end{aligned} \tag{A.48}$$

where we had to include also the explicit dependence on φ as it appears in the delta function. This result expresses the fully differential distribution in terms of the distribution differential only in the angle φ between \mathbf{k}_1 and \mathbf{k}_2 , and it will be used in Appendix B to construct simplified explicit expressions for the resummed contributions.

The key object that we need is thus

$$\begin{aligned} \frac{dC}{d\varphi}(z, \xi_1, \xi_2, Q^2, \varphi) &= \theta(Q^2 - 4m^2) \frac{1}{2} \frac{1}{2\pi} \sigma_0 \int d\psi \delta(\psi) \\ & \times \int d\phi_2(q; p, \bar{p}) |\mathcal{M}|^2, \end{aligned} \tag{A.49}$$

where $\sigma_0 = 16\pi^2 \alpha_s^2 / Q^2$, the factor $1/2$ is the flux factor and the $1/2\pi$ comes from the φ average. The matrix element squared $|\mathcal{M}|^2$ is given in Appendix 1. Note that because of the delta functions in Eq. (A.48) not all the variables of Eq. (A.49) are independent. In particular one can write $1/z = 1 + \xi_1 + \xi_2 + 2\sqrt{\xi_1 \xi_2} \cos \varphi$ and use it to fix one of them in terms of the others.

We now focus on the computation of $dC/d\varphi$. We observe that the two-body phase space Eq. (A.46) contains two delta functions corresponding to the mass shell condition of the heavy quarks. We write them in terms of the new variables, and get

$$0 = p^2 - m^2 = z_1 z_2 \frac{Q^2}{z} - |\mathbf{p}|^2 - m^2 \tag{A.50a}$$

$$\begin{aligned} 0 = \bar{p}^2 - m^2 &= (1 - z_1)(1 - z_2) \frac{Q^2}{z} - |\mathbf{q} - \mathbf{p}|^2 - m^2 \\ &= (1 - z_1 - z_2) \frac{Q^2}{z} - |\mathbf{q}|^2 + 2\mathbf{q} \cdot \mathbf{p}, \end{aligned} \tag{A.50b}$$

where in the last step we have used the first on-shell condition. The second condition contains a scalar product, and thus an angle, which is not ideal as this appears in the argument of

the delta function. In order to get rid of the scalar product, we use the first condition to fix z_2 , through the equation

$$z_2 = z \frac{|\mathbf{p}|^2 + m^2}{z_1 Q^2} \tag{A.51}$$

so that the second condition becomes

$$0 = \bar{p}^2 - m^2 = (1 - z_1) \frac{Q^2}{z} - \frac{|\mathbf{p}|^2 + m^2}{z_1} - |\mathbf{q}|^2 + 2\mathbf{q} \cdot \mathbf{p}, \tag{A.52}$$

We can now get rid of the scalar product by introducing a new vector $\mathbf{\Delta}$ defined by

$$\mathbf{p} = z_1 \mathbf{q} + \mathbf{\Delta} \tag{A.53}$$

so that

$$\begin{aligned} 0 = \bar{p}^2 - m^2 &= (1 - z_1) \frac{Q^2}{z} - \frac{|z_1 \mathbf{q} + \mathbf{\Delta}|^2 + m^2}{z_1} \\ & \quad - |\mathbf{q}|^2 + 2z_1 |\mathbf{q}|^2 + 2\mathbf{q} \cdot \mathbf{\Delta} \\ &= (1 - z_1) \left(\frac{Q^2}{z} - |\mathbf{q}|^2 \right) - \frac{|\mathbf{\Delta}|^2 + m^2}{z_1} \\ &= (1 - z_1) Q^2 - \frac{|\mathbf{\Delta}|^2 + m^2}{z_1}, \end{aligned} \tag{A.54}$$

that only depends on squared vectors (in the last step we have used $1 + \hat{q}_t^2 = \frac{1}{z}$). This can be now used to fix

$$|\mathbf{\Delta}|^2 = z_1(1 - z_1) Q^2 - m^2. \tag{A.55}$$

The two-body phase space can thus be rewritten as

$$\begin{aligned} & d\phi_2(q; p, \bar{p}) \\ &= \frac{d^4 p}{(2\pi)^3} \frac{d^4 \bar{p}}{(2\pi)^3} \delta(p^2 - m^2) \\ & \quad \times \delta(\bar{p}^2 - m^2) (2\pi)^4 \delta^{(4)}(q - p - \bar{p}) \theta(p^0) \theta(\bar{p}^0) \\ &= \frac{d^4 p}{4\pi^2} \delta(p^2 - m^2) \delta((q - p)^2 - m^2) \theta(p^0) \theta(q^0 - p^0) \\ &= \frac{Q^2}{8\pi^2 z} \delta\left(z_1 z_2 \frac{Q^2}{z} - |\mathbf{p}|^2 - m^2\right) \\ & \quad \times \delta\left((1 - z_1 - z_2) \frac{Q^2}{z} - |\mathbf{q}|^2 + 2\mathbf{q} \cdot \mathbf{p}\right) dz_1 dz_2 d^2 \mathbf{p} \\ & \quad \times \theta(z_1) \theta(z_2) \theta(1 - z_1) \theta(1 - z_2) \\ &= \frac{1}{8\pi^2} \delta\left((1 - z_1) Q^2 - \frac{|\mathbf{\Delta}|^2 + m^2}{z_1}\right) \\ & \quad \times \theta(z_1) \theta(1 - z_1) \frac{dz_1}{z_1} d^2 \mathbf{\Delta} \\ &= \frac{1}{16\pi^2} \theta\left(z_1(1 - z_1) Q^2 - m^2\right) dz_1 d\omega \end{aligned}$$

$$\begin{aligned}
 &= \frac{1}{16\pi^2} \theta \left(\sqrt{\frac{1}{4} - \frac{m^2}{Q^2}} - \left| \frac{1}{2} - z_1 \right| \right) dz_1 d\omega \\
 &= \frac{1}{16\pi^2} \sqrt{\frac{1}{4} - \frac{m^2}{Q^2}} \sin \beta d\beta d\omega
 \end{aligned} \tag{A.56}$$

where ω is the azimuthal angle of $\mathbf{\Delta}$ with respect to $\mathbf{k}_1 + \mathbf{k}_2$. Note that the condition $Q^2 > 4m^2$, needed to satisfy the theta function, is always verified in Eq. (A.49). If we wish to compute the z_1 integral numerically, it is convenient to change variable as

$$z_1 = \frac{1}{2} - \sqrt{\frac{1}{4} - \frac{m^2}{Q^2}} \cos \beta, \quad \beta \in [0, \pi] \tag{A.57}$$

which we used to obtain the last line of Eq. (A.56). Interestingly, in terms of these variables $|\mathbf{\Delta}|^2$ becomes

$$\begin{aligned}
 |\mathbf{\Delta}|^2 &= \frac{Q^2 - 4m^2}{4} \sin^2 \beta \\
 \Rightarrow |\mathbf{\Delta}| &= \frac{1}{2} \sqrt{Q^2 - 4m^2} \sin \beta,
 \end{aligned} \tag{A.58}$$

where we do not need to include an absolute value, as in the allowed range $\sin \beta$ is always positive.

The form of the phase space Eq. (A.56) is very convenient from a numerical point of view. To be able to perform all integrations, we also need to express the matrix element squared appearing in Eq. (A.49) in terms of the variables β (or z_1) and ω . We start by rewriting

$$\begin{aligned}
 z_2 &= z \frac{|z_1 \mathbf{q} + \mathbf{\Delta}|^2 + m^2}{z_1 Q^2} \\
 &= z \frac{z_1^2 |\mathbf{q}|^2 + |\mathbf{\Delta}|^2 + 2z_1 \mathbf{q} \cdot \mathbf{\Delta} + m^2}{z_1 Q^2} \\
 &= z \left[1 - z_1(1 - \hat{q}_t^2) + 2\sqrt{\hat{q}_t^2} \sqrt{z_1(1 - z_1) - m^2/Q^2} \cos(\omega - \psi) \right] \\
 &= z \left[1 - (1 - \hat{q}_t^2) \left(\frac{1}{2} - \sqrt{\frac{1}{4} - \frac{m^2}{Q^2}} \cos \beta \right) \right. \\
 &\quad \left. + \sqrt{\hat{q}_t^2} \sqrt{1 - 4m^2/Q^2} \sin \beta \cos(\omega - \psi) \right]
 \end{aligned} \tag{A.59}$$

where $\psi = 0$ for our choice of variables, Eq. (A.42). Finally, we will see in Appendix A.3 that the matrix element depends on the scalar product $\mathbf{k}_2 \cdot \mathbf{p}$ through the variables T Eq. (A.67c) and U Eq. (A.67d). We can write

$$\begin{aligned}
 \frac{\mathbf{k}_2 \cdot \mathbf{p}}{Q^2} &= \frac{\mathbf{k}_2 \cdot (z_1 \mathbf{q} + \mathbf{\Delta})}{Q^2} \\
 &= \frac{z_1(\mathbf{k}_2^2 + \mathbf{k}_2 \cdot \mathbf{k}_1) + \mathbf{k}_2 \cdot \mathbf{\Delta}}{Q^2}
 \end{aligned}$$

$$= z_1 \xi_2 + z_1 \sqrt{\xi_1 \xi_2} \cos \varphi + \sqrt{\xi_2} \sqrt{\frac{1}{4} - \frac{m^2}{Q^2}} \sin \beta \cos \omega', \tag{A.60}$$

where ω' is the angle between $\mathbf{\Delta}$ and \mathbf{k}_2 . It is given by $\omega' = \omega + \varphi'$, where φ' is the angle of $\mathbf{q} = \mathbf{k}_1 + \mathbf{k}_2$ with respect to \mathbf{k}_2 , given in Eq. (A.40). For the on-shell limit $\xi_2 \rightarrow 0$ it is also useful to write

$$\hat{p}_t^2 \equiv \frac{\mathbf{p}^2}{Q^2} = z_1^2 \xi_1 + \frac{|\mathbf{\Delta}|^2}{Q^2} + 2z_1 \sqrt{\xi_1} \frac{|\mathbf{\Delta}|}{Q} \cos \omega \tag{A.61}$$

in terms of the new phase-space variables. In the fully on-shell limit the result simplifies further

$$\hat{p}_t^2 = \frac{|\mathbf{\Delta}|^2}{Q^2} = z_1(1 - z_1) - \frac{m^2}{Q^2}. \tag{A.62}$$

A.3 Matrix element

In this Appendix we report the matrix element squared for heavy quark pair production from two off-shell gluons. This has been computed in Refs. [27, 52]. Here, we rewrite that result in terms of the variables that we have defined above.

The matrix element is separated into an abelian and a non-abelian parts as

$$|\mathcal{M}|^2 = \frac{1}{2C_A} |\mathcal{M}|_{\text{ab}}^2 + \frac{1}{4C_F} |\mathcal{M}|_{\text{nab}}^2 \tag{A.63}$$

with

$$\begin{aligned}
 |\mathcal{M}|_{\text{ab}}^2 &= \frac{1}{z^2} \\
 &\times \left[\frac{1}{TU} - \frac{1}{\xi_1 \xi_2} \left(1 + \frac{z_2(1 - z_1)}{zT} + \frac{z_1(1 - z_2)}{zU} \right)^2 \right]
 \end{aligned} \tag{A.64}$$

and

$$\begin{aligned}
 |\mathcal{M}|_{\text{nab}}^2 &= \frac{1}{z^2} \left[-\frac{1}{TU} + \frac{2z}{S} + \frac{(T - U)(z_1 - z_2)}{STU} \right. \\
 &\quad \left. + \frac{2}{\xi_1 \xi_2} \left(\frac{1}{2} + \frac{z_2(1 - z_1)}{zT} - \frac{\Delta}{S} \right) \right. \\
 &\quad \left. \times \left(\frac{1}{2} + \frac{z_1(1 - z_2)}{zU} + \frac{\Delta}{S} \right) \right],
 \end{aligned} \tag{A.65}$$

where

$$\begin{aligned}
 \Delta &= \frac{z_1(1 - z_2)}{z} - \frac{z_2(1 - z_1)}{z} + \xi_1 z_2 - \xi_2 z_1 \\
 &\quad + \frac{z_2 - z_1}{2z} + \frac{\mathbf{p} \cdot (\mathbf{k}_2 - \mathbf{k}_1)}{Q^2}
 \end{aligned} \tag{A.66}$$

and

$$S = \frac{\hat{s}}{Q^2} = \frac{(k_1 + k_2)^2}{Q^2} = \frac{1}{z} - \xi_1 - \xi_2 - 2\sqrt{\xi_1 \xi_2} \cos \varphi \tag{A.67a}$$

$$T = \frac{t - m^2}{Q^2} = \frac{(p - k_1)^2 - m^2}{Q^2} = \frac{2\mathbf{k}_1 \cdot \mathbf{p}}{Q^2} - \xi_1 - \frac{z_2}{z} \tag{A.67b}$$

$$= \frac{(\bar{p} - k_2)^2 - m^2}{Q^2} = -\frac{2\mathbf{k}_2 \cdot \mathbf{p}}{Q^2} + \xi_2 + 2\sqrt{\xi_1 \xi_2} \cos \varphi - \frac{1 - z_1}{z} \tag{A.67c}$$

$$U = \frac{u - m^2}{Q^2} = \frac{(p - k_2)^2 - m^2}{Q^2} = \frac{2\mathbf{k}_2 \cdot \mathbf{p}}{Q^2} - \xi_2 - \frac{z_1}{z} \tag{A.67d}$$

$$= \frac{(\bar{p} - k_1)^2 - m^2}{Q^2} = -\frac{2\mathbf{k}_1 \cdot \mathbf{p}}{Q^2} + \xi_1 + 2\sqrt{\xi_1 \xi_2} \cos \varphi - \frac{1 - z_2}{z}. \tag{A.67e}$$

Note that in the case of the pair kinematics, where $q = p + \bar{p}$, we have $\hat{s} = Q^2$ and thus $S = 1$. We can use the expressions of T and U to rewrite

$$\frac{\mathbf{p} \cdot (\mathbf{k}_2 - \mathbf{k}_1)}{Q^2} = \frac{1}{2} \left[U - T + \xi_2 - \xi_1 + \frac{z_1 - z_2}{z} \right] \tag{A.68}$$

so that Δ simplifies to

$$\Delta = \frac{z_1 - z_2}{z} + \xi_1 z_2 - \xi_2 z_1 + \frac{U + \xi_2 - T - \xi_1}{2}. \tag{A.69}$$

We also recall the relation

$$\hat{s} + t + u = 2m^2 - |\mathbf{k}_1|^2 - |\mathbf{k}_2|^2, \tag{A.70}$$

namely

$$S + T + U + \xi_1 + \xi_2 = 0. \tag{A.71}$$

Thus, one can always express one of these variables in terms of the other four.

Note that the matrix element squared is symmetric under the simultaneous exchange

$$\mathbf{k}_1 \leftrightarrow \mathbf{k}_2, \quad z_1 \leftrightarrow z_2. \tag{A.72}$$

This implies that, in the pair kinematics, after integrating over the two z_1 and z_2 variables (which appear symmetrically in the phase space) the off-shell coefficient is symmetric under the exchange of the two gluon virtualities. Similarly, in the single-quark kinematics, the off-shell coefficient is symmetric under the exchange of the two gluon virtualities and a sign change in the rapidity η .

A.4 On-shell limit

The resummation discussed in Sect. 2.3 requires also the coefficient function with just one gluon off-shell. This result can be obtained by simply taking the partial on-shell limit, say $\mathbf{k}_2 \rightarrow 0$, of the fully off-shell result. Here we perform this limit at the level of the matrix element squared. We will also compute the fully on-shell limit, needed for the fixed-order expansion, which also serves as a cross check.

When taking the on-shell limit, one must be careful in the choice of the parameters used to write the matrix element. Previously, we have used the most convenient variables to obtain a compact form, but some of them are not independent of the others. When taking an on-shell limit, any such relation must be made explicit.

We commented at the beginning of this appendix that the off-shell coefficient depends on 7 independent variables, 4 initial-state ones and 3 final-state ones. Since the matrix element is dimensionless, we shall conveniently choose a set of dimensionless variables. Thus, for the initial state we use the variables z, ξ_1, ξ_2, φ defined in Eq. (A.6), while for the final state we could consider any three variables out of $\vartheta, \hat{p}_t, z_1, z_2$, namely

$$\vartheta, \hat{p}_t, z_1 \quad \text{or} \quad \vartheta, \hat{p}_t, z_2 \quad \text{or} \quad \vartheta, z_1, z_2 \quad \text{or} \quad \hat{p}_t, z_1, z_2. \tag{A.73}$$

The relation between these four variables is given by the equation

$$\hat{p}_t = \frac{\frac{z_1+z_2-1}{z} + \xi_1 + \xi_2 + 2\sqrt{\xi_1 \xi_2} \cos \varphi}{2\sqrt{\xi_1 + \xi_2 + 2\sqrt{\xi_1 \xi_2} \cos \varphi} \cos \vartheta}, \tag{A.74}$$

which descends from the on-shell condition $p^2 = \bar{p}^2 (= m^2)$. All these choices are acceptable provided they are kept throughout the computation of the on-shell limit. Once the on-shell limit $\mathbf{k}_2 \rightarrow 0$ is taken, we must also compute the average over φ (as it is no longer well defined), so that the remaining variables upon which the matrix element can be expressed are just 5, e.g. $z, \xi_1, \vartheta, z_1, z_2$ or $z, \xi_1, \hat{p}_t, z_1, z_2$. If we also want to compute the fully on-shell limit $\mathbf{k}_{1,2} \rightarrow 0$, the azimuthal angle of \mathbf{p} becomes arbitrary, and the result depends on just 3 independent variables, z, \hat{p}_t, z_1 or z, \hat{p}_t, z_2 (not z, z_1, z_2 because they are no longer independent in the on-shell case). Therefore, it is convenient to have \hat{p}_t in our variable set, so we discard the third set of Eq. (A.73). The most convenient set is probably the last, \hat{p}_t, z_1, z_2 , so we go for it.

When looking at the matrix element squared, Eqs. (A.64) and (A.65), it is clear that there is a potential singularity in the on-shell limit due to the presence of a factor $1/\xi_2$. This is harmless if the terms in rounded brackets are of order $\sqrt{\xi_2}$.

To prove this, we first expand S, T, U at small ξ_2 . From the representations of Eqs. (A.67a), (A.67c) and (A.67d) we get immediately

$$S = \frac{1}{z} - \xi_1 - 2\sqrt{\xi_1\xi_2} \cos \varphi + \mathcal{O}(\xi_2) \tag{A.75a}$$

$$T = -\frac{1-z_1}{z} + 2\sqrt{\xi_1\xi_2} \cos \varphi - 2\sqrt{\hat{p}_t^2\xi_2} \cos(\vartheta' - \varphi) + \mathcal{O}(\xi_2) \tag{A.75b}$$

$$U = -\frac{z_1}{z} + 2\sqrt{\hat{p}_t^2\xi_2} \cos(\vartheta' - \varphi) + \mathcal{O}(\xi_2), \tag{A.75c}$$

where ϑ' is the angle of \mathbf{p} with respect to \mathbf{k}_1 , which coincides with ϑ in the on-shell limit $\mathbf{k}_2 \rightarrow 0$.

Let us start from the abelian part of the matrix element, Eq. (A.64). Expanding the rounded brackets at small ξ_2 , we find

$$\begin{aligned} & 1 + \frac{z_2(1-z_1)}{zT} + \frac{z_1(1-z_2)}{zU} \\ &= 1 - \frac{z_2}{1 - \frac{z}{1-z_1} \left(2\sqrt{\xi_1\xi_2} \cos \varphi - 2\sqrt{\xi_2\hat{p}_t^2} \cos(\vartheta' - \varphi) \right)} \\ & - \frac{1-z_2}{1 - \frac{z}{z_1} 2\sqrt{\xi_2\hat{p}_t^2} \cos(\vartheta' - \varphi)} + \mathcal{O}(\xi_2) \\ &= -2z\sqrt{\xi_2} \left[\frac{z_2}{1-z_1} \sqrt{\xi_1} \cos \varphi + \left(\frac{1-z_2}{z_1} - \frac{z_2}{1-z_1} \right) \right. \\ & \left. \times \sqrt{\hat{p}_t^2} \cos(\vartheta' - \varphi) \right] + \mathcal{O}(\xi_2), \tag{A.76} \end{aligned}$$

which is indeed of order $\sqrt{\xi_2}$. Averaging over φ , the abelian part of the matrix element squared becomes

$$\begin{aligned} |\mathcal{M}|_{\text{ab}}^2 \stackrel{\mathbf{k}_2 \rightarrow 0}{=} & \int_0^{2\pi} \frac{d\varphi}{2\pi} \frac{1}{z^2} \left[\frac{1}{TU} - \frac{4z^2}{\xi_1} \left(\frac{z_2}{1-z_1} \sqrt{\xi_1} \cos \varphi \right. \right. \\ & \left. \left. + \left(\frac{1-z_2}{z_1} - \frac{z_2}{1-z_1} \right) \sqrt{\hat{p}_t^2} \cos(\vartheta' - \varphi) \right)^2 \right] \\ &= \frac{1}{z_1(1-z_1)} - \frac{2}{\xi_1} \left[\left(\frac{z_2}{1-z_1} \right)^2 \xi_1 \right. \\ & \left. + \left(\frac{1-z_2}{z_1} - \frac{z_2}{1-z_1} \right)^2 \hat{p}_t^2 \right. \\ & \left. + \frac{z_2}{1-z_1} \left(\frac{1-z_2}{z_1} - \frac{z_2}{1-z_1} \right) 2\sqrt{\xi_1\hat{p}_t^2} \cos \vartheta \right], \tag{A.77} \end{aligned}$$

where we have replaced ϑ' with ϑ as they now coincide. Note that we are using more variables than needed. Indeed, using Eq. (A.74) we can rewrite $\cos \vartheta$ in terms of other variables. In particular, in the $\xi_2 \rightarrow 0$ limit it is easy to obtain from Eq. (A.74) the relation

$$2\sqrt{\xi_1\hat{p}_t^2} \cos \vartheta = \frac{z_1+z_2-1}{z} + \xi_1, \tag{A.78}$$

from which we finally find

$$\begin{aligned} |\mathcal{M}|_{\text{ab}}^2 \stackrel{\mathbf{k}_2 \rightarrow 0}{=} & \frac{1-2z_2(1-z_2)}{z_1(1-z_1)} - \frac{2}{\xi_1} \\ & \times \left(\frac{1-z_1-z_2}{z_1(1-z_1)} \right)^2 \left[\hat{p}_t^2 - \frac{z_1z_2}{z} \right]. \tag{A.79} \end{aligned}$$

For the non-abelian part, Eq. (A.65), let us start by expanding Δ , Eq. (A.69), to order $\sqrt{\xi_2}$:

$$\begin{aligned} \Delta = & \left(\xi_1 - \frac{1}{z} \right) \left(z_2 - \frac{1}{2} \right) \\ & + \sqrt{\xi_2} \left(2\sqrt{\hat{p}_t^2} \cos(\vartheta' - \varphi) - \sqrt{\xi_1} \cos \varphi \right) \\ & + \mathcal{O}(\xi_2). \tag{A.80} \end{aligned}$$

The rounded brackets of Eq. (A.65) become

$$\begin{aligned} \frac{1}{2} + \frac{z_2(1-z_1)}{zT} - \frac{\Delta}{S} &= 2z\sqrt{\xi_2} \left[\left(\frac{z_2}{1-z\xi_1} - \frac{z_2}{1-z_1} \right) \sqrt{\xi_1} \cos \varphi - \left(\frac{1}{1-z\xi_1} - \frac{z_2}{1-z_1} \right) \sqrt{\hat{p}_t^2} \cos(\vartheta' - \varphi) \right] + \mathcal{O}(\xi_2) \\ \frac{1}{2} + \frac{z_1(1-z_2)}{zU} + \frac{\Delta}{S} &= 2z\sqrt{\xi_2} \left[-\frac{z_2}{1-z\xi_1} \sqrt{\xi_1} \cos \varphi + \left(\frac{1}{1-z\xi_1} - \frac{1-z_2}{z_1} \right) \sqrt{\hat{p}_t^2} \cos(\vartheta' - \varphi) \right] + \mathcal{O}(\xi_2), \tag{A.81} \end{aligned}$$

so that we can finally find the partial on-shell limit of the non-abelian part of the matrix element,

$$\begin{aligned}
 |\mathcal{M}|_{\text{nab}}^2 \stackrel{\mathbf{k}_2 \rightarrow 0}{=} & \int_0^{2\pi} \frac{d\varphi}{2\pi} \left\{ -\frac{1}{z^2 T U} + \frac{2}{z S} + \frac{(T-U)(z_1-z_2)}{z^2 S T U} + \frac{8}{\xi_1} \left[\left(\frac{z_2}{1-z\xi_1} - \frac{z_2}{1-z_1} \right) \sqrt{\xi_1} \cos \varphi \right. \right. \\
 & \left. \left. - \left(\frac{1}{1-z\xi_1} - \frac{z_2}{1-z_1} \right) \sqrt{\hat{p}_t^2} \cos(\vartheta' - \varphi) \right] \left[-\frac{z_2}{1-z\xi_1} \sqrt{\xi_1} \cos \varphi + \left(\frac{1}{1-z\xi_1} - \frac{1-z_2}{z_1} \right) \times \sqrt{\hat{p}_t^2} \cos(\vartheta' - \varphi) \right] \right\} \\
 & = -\frac{1}{z_1(1-z_1)} + \frac{2}{1-z\xi_1} + \frac{(1-2z_1)(z_2-z_1)}{z_1(1-z_1)(1-z\xi_1)} + \frac{4}{\xi_1(1-z\xi_1)^2} \left[\frac{(z_1-z\xi_1)z_2^2}{1-z_1} \xi_1 - \left(1 - \frac{z_2(1-z\xi_1)}{1-z_1} \right) \right. \\
 & \left. \times \left(1 - \frac{(1-z_2)(1-z\xi_1)}{z_1} \right) \hat{p}_t^2 + \left\{ \left(1 - \frac{1-z\xi_1}{1-z_1} \right) \left(1 - \frac{(1-z_2)(1-z\xi_1)}{z_1} \right) + 1 - \frac{z_2(1-z\xi_1)}{1-z_1} \right\} z_2 \sqrt{\xi_1} \hat{p}_t^2 \cos \vartheta \right]. \tag{A.82}
 \end{aligned}$$

Using again Eq. (A.78) we finally get

$$\begin{aligned}
 |\mathcal{M}|_{\text{nab}}^2 = & -\frac{1}{z_1(1-z_1)} + \frac{2}{1-z\xi_1} + \frac{(1-2z_1)(z_2-z_1)}{z_1(1-z_1)(1-z\xi_1)} + \frac{2z_2}{(1-z\xi_1)^2} \left[2 \frac{(z_1-z\xi_1)z_2}{1-z_1} + \left(1 - \frac{1-z\xi_1}{1-z_1} \right) \right. \\
 & \left. \times \left(1 - \frac{(1-z_2)(1-z\xi_1)}{z_1} \right) + 1 - \frac{z_2(1-z\xi_1)}{1-z_1} \right] + \frac{2}{\xi_1(1-z\xi_1)^2} \left[-2 \left(1 - \frac{z_2(1-z\xi_1)}{1-z_1} \right) \right. \\
 & \left. \times \left(1 - \frac{(1-z_2)(1-z\xi_1)}{z_1} \right) \hat{p}_t^2 + \left\{ \left(1 - \frac{1-z\xi_1}{1-z_1} \right) \left(1 - \frac{(1-z_2)(1-z\xi_1)}{z_1} \right) \right. \right. \\
 & \left. \left. + 1 - \frac{z_2(1-z\xi_1)}{1-z_1} \right\} z_2 \frac{z_1+z_2-1}{z} \right]. \tag{A.83}
 \end{aligned}$$

We can now further take the limit $\mathbf{k}_1 \rightarrow 0$ to obtain the fully on-shell result. This is useful as a cross-check as it must coincide with the on-shell computation, see e.g. [62]. In the on-shell limit, z, z_1 and z_2 are no longer independent, as one can see from Eq. (A.78). Moreover, the angle ϑ becomes arbitrary (the reference vector \mathbf{k}_1 does not exist anymore), so an average over ϑ must be taken. From Eq. (A.78) we can write

$$z_2 = 1 - z_1 + 2z \sqrt{\hat{p}_t^2 \xi_1} \cos \vartheta + \mathcal{O}(\xi_1) \tag{A.84}$$

from which we find

$$\begin{aligned}
 |\mathcal{M}|_{\text{ab}}^2 \stackrel{\mathbf{k}_{1,2} \rightarrow 0}{=} & \frac{1}{z_1(1-z_1)} \\
 & \times \left[1 + 4z \hat{p}_t^2 \left(1 - \frac{z \hat{p}_t^2}{z_1(1-z_1)} \right) \right] - 2 \tag{A.85}
 \end{aligned}$$

$$|\mathcal{M}|_{\text{nab}}^2 \stackrel{\mathbf{k}_{1,2} \rightarrow 0}{=} 4z_1(1-z_1) - 2 - 8z \hat{p}_t^2 \left(1 - \frac{z \hat{p}_t^2}{z_1(1-z_1)} \right), \tag{A.86}$$

where we can also write $\hat{p}_t^2 = \frac{z_1(1-z_1)}{z} - \frac{m^2}{Q^2}$. We have verified that this result is in agreement with on-shell computations [62]. For completeness, we also report the on-shell matrix element for the $q\bar{q}$ channel:

$$|\mathcal{M}|_{q\bar{q}}^2 = \frac{C_F}{C_A} \left(1 - 2z \hat{p}_t^2 \right). \tag{A.87}$$

Appendix B: Simplifications in the resummation formulae for pair kinematics

When considering pair kinematics we fix $q \equiv p + \bar{p}$. Because of momentum conservation, we also have $q = k_1 + k_2$. Therefore, each component of q is fixed in terms of the initial state variables. It follows that the off-shell coefficient function factorizes as in Eq. (A.48), that we report here for convenience

$$\begin{aligned}
 & \frac{Q^4 d\mathcal{C}}{dQ^2 d\eta dq_t^2 d\varphi}(z, \xi_1, \xi_2, Q^2, \eta, q_t^2, \varphi) \\
 & = \frac{d\mathcal{C}}{d\varphi}(z, \xi_1, \xi_2, Q^2, \varphi) \delta \left(1 + \hat{q}_t^2 - \frac{1}{z} \right) \delta(\eta) \\
 & \quad \times \delta \left(\hat{q}_t^2 - \xi_1 - \xi_2 - 2\sqrt{\xi_1 \xi_2} \cos \varphi \right), \tag{B.1}
 \end{aligned}$$

where the differential coefficient is given in terms of a more integrated one times three delta functions. These delta functions can be used to compute the integrations in the resummation formulae of Sect. 2.3. In this appendix, we exploit this to present simplified resummed expressions, that we have implemented in the numerical code HELL.

From Eq. (B.1) we can obtain immediately the triple differential off-shell coefficient function by integrating in φ using the last delta function

$$\begin{aligned} & \frac{Q^4 dC}{dQ^2 d\eta dq_t^2}(z, \xi_1, \xi_2, Q^2, \eta, q_t^2) \\ &= \frac{\theta\left(1 - \left|\frac{\hat{q}_t^2 - \xi_1 - \xi_2}{2\sqrt{\xi_1 \xi_2}}\right|\right)}{\sqrt{4\xi_1 \xi_2 - (\hat{q}_t^2 - \xi_1 - \xi_2)^2}} \delta\left(1 + \hat{q}_t^2 - \frac{1}{z}\right) \delta(\eta) \\ & \times \left[\frac{dC}{d\varphi}(z, \xi_1, \xi_2, Q^2, \bar{\varphi}) \right. \\ & \left. + \frac{dC}{d\varphi}(z, \xi_1, \xi_2, Q^2, 2\pi - \bar{\varphi}) \right] \end{aligned} \tag{B.2}$$

$$\bar{\varphi} = \cos^{-1} \frac{\hat{q}_t^2 - \xi_1 - \xi_2}{2\sqrt{\xi_1 \xi_2}}, \quad 0 \leq \bar{\varphi} \leq \pi, \tag{B.3}$$

where the φ -differential distribution is evaluated at specific values of φ . Note however that integrating over φ immediately is not always the best strategy. For instance, when we take the partial on-shell limit $\xi_2 \rightarrow 0$ we obtain

$$\begin{aligned} & \frac{Q^4 dC}{dQ^2 d\eta dq_t^2 d\varphi}(z, \xi_1, 0, Q^2, \eta, q_t^2, \varphi) = \frac{dC}{d\varphi}(z, \xi_1, 0, Q^2, \varphi) \\ & \times \delta\left(1 + \hat{q}_t^2 - \frac{1}{z}\right) \delta(\eta) \delta(\hat{q}_t^2 - \xi_1), \end{aligned} \tag{B.4}$$

$$\begin{aligned} & \frac{Q^4 dC_{\text{aux}\pm}}{dQ^2 dy dq_t^2} \left(x, Q^2, y, q_t^2, \alpha_s, \frac{Q^2}{\mu_F^2}\right) = \frac{1}{1 + \hat{q}_t^2} C\left(\frac{1}{1 + \hat{q}_t^2}, \hat{q}_t^2, 0, Q^2\right) \delta\left(y \pm \frac{1}{2} \log \frac{1}{x(1 + \hat{q}_t^2)}\right) \\ & \left\{ \alpha_s(\mu_F^2) P_0(x(1 + \hat{q}_t^2)) \left(\frac{1}{\hat{q}_t^2}\right)_+ + \alpha_s^2(\mu_F^2) \left[P_1(x(1 + \hat{q}_t^2)) \left(\frac{1}{\hat{q}_t^2}\right)_+ \right. \right. \\ & \left. \left. + (P_{00}(x(1 + \hat{q}_t^2)) - \beta_0 P_0(x(1 + \hat{q}_t^2))) \left(\frac{\log \frac{q_t^2}{\mu_F^2}}{\hat{q}_t^2}\right)_+ \right] + \mathcal{O}(\alpha_s^3) \right\}. \end{aligned} \tag{B.7}$$

where the delta functions do not depend on φ anymore, thus making its integration trivial

$$\begin{aligned} & \frac{Q^4 dC}{dQ^2 d\eta dq_t^2}(z, \xi_1, 0, Q^2, \eta, q_t^2) \\ &= C(z, \xi_1, 0, Q^2) \delta\left(1 + \hat{q}_t^2 - \frac{1}{z}\right) \delta(\eta) \delta(\hat{q}_t^2 - \xi_1). \end{aligned} \tag{B.5}$$

This result is needed for the auxiliary function Eq. (2.35), and also for the subtraction of the plus distributions in the perturbative expansion of the resummed result, see Sect. 2.4.

We can now use these results in the resummation formulae, using the delta functions to perform integrations explicitly when possible. As far as the auxiliary function Eq. (2.35) is concerned, we can start from Eq. (B.5) and use the $\delta(\hat{q}_t^2 - \xi_1)$ to compute the ξ_1 integration. The result is

$$\begin{aligned} & \frac{Q^4 dC_{\text{aux}\pm}}{dQ^2 dy dq_t^2} \left(x, Q^2, y, q_t^2, \alpha_s, \frac{Q^2}{\mu_F^2}\right) = \frac{1}{1 + \hat{q}_t^2} \\ & \times C\left(\frac{1}{1 + \hat{q}_t^2}, \hat{q}_t^2, 0, Q^2\right) U'_{\text{reg}}(x(1 + \hat{q}_t^2), q_t^2, \mu_F^2) \\ & \times \delta\left(y \pm \frac{1}{2} \log \frac{1}{x(1 + \hat{q}_t^2)}\right), \end{aligned} \tag{B.6}$$

which does not contain any further integration. Note the presence of a delta function in the result, which can be used in the cross section to integrate over parton distributions. The fixed-order expansion of Eq. (B.6) is given according to Eq. (2.40) by

We observe that, for this auxiliary function, the expansion is a distribution in q_t^2 . This is not an issue: the triple differential distribution is interesting only for non-zero values of q_t^2 , and indeed any measurement will require a q_t^2 greater than some resolution cutoff. Should one be interested in integrating over q_t^2 down to zero, either to compute the integrated distribution or to obtain a binned version of the q_t^2 distribution, one has simply to take care of using the plus distribution in the integration.

We now move to the regular function Eq. (2.34). We get

$$\begin{aligned} \frac{Q^4 dC_{\text{reg}}}{dQ^2 dy dq_t^2} \left(x, Q^2, y, q_t^2, \alpha_s, \frac{Q^2}{\mu_F^2} \right) &= \frac{1}{1 + \hat{q}_t^2} \int_0^\infty d\xi_1 \int_0^\infty d\xi_2 \int_0^{2\pi} d\varphi \frac{dC}{d\varphi} \left(\frac{1}{1 + \hat{q}_t^2}, \xi_1, \xi_2, Q^2, \varphi \right) \\ &\times U'_{\text{reg}} \left(\sqrt{x(1 + \hat{q}_t^2)} e^y, Q^2 \xi_1, \mu_F^2 \right) U'_{\text{reg}} \left(\sqrt{x(1 + \hat{q}_t^2)} e^{-y}, Q^2 \xi_2, \mu_F^2 \right) \delta \left(\hat{q}_t^2 - \xi_1 - \xi_2 - 2\sqrt{\xi_1 \xi_2} \cos \varphi \right) \\ &\times \theta \left(\frac{e^{-2|y|}}{x} - 1 - \hat{q}_t^2 \right) \end{aligned} \tag{B.8}$$

$$\begin{aligned} &= \frac{\theta \left(\frac{e^{-2|y|}}{x} - 1 - \hat{q}_t^2 \right)}{1 + \hat{q}_t^2} \int_0^\infty d\xi_1 \int_0^\infty d\xi_2 \frac{\theta \left(1 - \left| \frac{\hat{q}_t^2 - \xi_1 - \xi_2}{2\sqrt{\xi_1 \xi_2}} \right| \right)}{\sqrt{4\xi_1 \xi_2 - (\hat{q}_t^2 - \xi_1 - \xi_2)^2}} U'_{\text{reg}} \left(\sqrt{x(1 + \hat{q}_t^2)} e^y, Q^2 \xi_1, \mu_F^2 \right) \\ &\times U'_{\text{reg}} \left(\sqrt{x(1 + \hat{q}_t^2)} e^{-y}, Q^2 \xi_2, \mu_F^2 \right) \left[\frac{dC}{d\varphi} \left(\frac{1}{1 + \hat{q}_t^2}, \xi_1, \xi_2, Q^2, \bar{\varphi} \right) + \frac{dC}{d\varphi} \left(\frac{1}{1 + \hat{q}_t^2}, \xi_1, \xi_2, Q^2, 2\pi - \bar{\varphi} \right) \right], \end{aligned} \tag{B.9}$$

where we have used Eq. (B.1) in the first step and Eq. (B.2) in the second step. Note that the theta function inside the integration can be recast in the (physically obvious) constraint

$$\left(\sqrt{\xi_1} - \sqrt{\xi_2} \right)^2 \leq \hat{q}_t^2 \leq \left(\sqrt{\xi_1} + \sqrt{\xi_2} \right)^2. \tag{B.10}$$

The integration over $\xi_{1,2}$ shall be performed numerically. The fixed-order expansion of Eq. (B.9) can be computed according to Eq. (2.39). To this end, it is better to start from Eq. (B.8), to obtain

This result is not immediately usable as delta functions still appear explicitly, and the cancellation of singularities in $\xi_1, \xi_2 = 0$ requires integrating over these delta functions in a proper order.

To do so, we make some observations. First, when ξ_1 or ξ_2 is zero, the coefficient does no longer depend on φ in principle. However, when considering the limit $\xi_{1,2} \rightarrow 0$, a dependence on φ remains. So, for later convenience, we keep the last argument having in mind a limit procedure. Second,

$$\begin{aligned} \frac{Q^4 dC_{\text{reg}}}{dQ^2 dy dq_t^2} \left(x, Q^2, y, q_t^2, \alpha_s, \frac{Q^2}{\mu_F^2} \right) &= \frac{1}{1 + \hat{q}_t^2} \int_0^\infty d\xi_1 \int_0^\infty d\xi_2 \int_0^{2\pi} d\varphi \frac{dC}{d\varphi} \left(\frac{1}{1 + \hat{q}_t^2}, \xi_1, \xi_2, Q^2, \varphi \right) \\ &\times \left[\alpha_s^2(\mu_F^2) \left(\frac{1}{\xi_1} \right)_+ \left(\frac{1}{\xi_2} \right)_+ P_0 \left(\sqrt{x(1 + \hat{q}_t^2)} e^y \right) P_0 \left(\sqrt{x(1 + \hat{q}_t^2)} e^{-y} \right) + \mathcal{O}(\alpha_s^3) \right] \\ &\times \delta \left(\hat{q}_t^2 - \xi_1 - \xi_2 - 2\sqrt{\xi_1 \xi_2} \cos \varphi \right) \theta \left(\frac{e^{-2|y|}}{x} - 1 - \hat{q}_t^2 \right) \end{aligned} \tag{B.11}$$

$$= \frac{1}{1 + \hat{q}_t^2} \theta \left(\frac{e^{-2|y|}}{x} - 1 - \hat{q}_t^2 \right) \left[\alpha_s^2(\mu_F^2) P_0 \left(\sqrt{x(1 + \hat{q}_t^2)} e^y \right) P_0 \left(\sqrt{x(1 + \hat{q}_t^2)} e^{-y} \right) + \mathcal{O}(\alpha_s^3) \right] \int_0^{2\pi} d\varphi I \tag{B.12}$$

having defined

$$\begin{aligned} I &= \int_0^\infty \frac{d\xi_1}{\xi_1} \int_0^\infty \frac{d\xi_2}{\xi_2} \left[\frac{dC}{d\varphi} \left(\frac{1}{1 + \hat{q}_t^2}, \xi_1, \xi_2, Q^2, \varphi \right) \right. \\ &\times \delta \left(\hat{q}_t^2 - \xi_1 - \xi_2 - 2\sqrt{\xi_1 \xi_2} \cos \varphi \right) \\ &- \frac{dC}{d\varphi} \left(\frac{1}{1 + \hat{q}_t^2}, \xi_1, 0, Q^2, \varphi \right) \delta \left(\hat{q}_t^2 - \xi_1 \right) \theta(1 - \xi_2) \\ &- \frac{dC}{d\varphi} \left(\frac{1}{1 + \hat{q}_t^2}, 0, \xi_2, Q^2, \varphi \right) \delta \left(\hat{q}_t^2 - \xi_2 \right) \theta(1 - \xi_1) \\ &\left. + \frac{dC}{d\varphi} \left(\frac{1}{1 + \hat{q}_t^2}, 0, 0, Q^2, \varphi \right) \delta \left(\hat{q}_t^2 \right) \theta(1 - \xi_1) \theta(1 - \xi_2) \right] \end{aligned} \tag{B.13}$$

the last term is proportional to $\delta(\hat{q}_t^2)$, which is zero everywhere in the \hat{q}_t^2 distribution, except for a single point. This point is interesting only for computing the cumulative distribution between $\hat{q}_t^2 = 0$ and some given value, but in this case it is more convenient to consider the integrated distribution and subtract from it the integral from that value to infinity. Therefore, for our purposes, we can assume $\hat{q}_t^2 > 0$ and ignore the last line. Finally, we observe that the integrand is symmetric for the exchange $\xi_1 \leftrightarrow \xi_2$, as a consequence of the analogous symmetry of the function $dC/d\varphi$.

We can separate the integration region into 4 subregions, divided by the lines $\xi_1 = 1$ and $\xi_2 = 1$. As a result we can write

$$I = I_1 + I_2 + I_3 + I_4 \tag{B.14}$$

$$I_1 = \int_0^1 \frac{d\xi_1}{\xi_1} \int_0^1 \frac{d\xi_2}{\xi_2} \left[\frac{dC}{d\varphi} \left(\frac{1}{1 + \hat{q}_t^2}, \xi_1, \xi_2, Q^2, \varphi \right) \delta \left(\hat{q}_t^2 - \xi_1 - \xi_2 - 2\sqrt{\xi_1 \xi_2} \cos \varphi \right) - \frac{dC}{d\varphi} \left(\frac{1}{1 + \hat{q}_t^2}, \xi_1, 0, Q^2 \right) \delta \left(\hat{q}_t^2 - \xi_1 \right) - \frac{dC}{d\varphi} \left(\frac{1}{1 + \hat{q}_t^2}, 0, \xi_2, Q^2 \right) \delta \left(\hat{q}_t^2 - \xi_2 \right) \right] \tag{B.15}$$

$$I_2 = \int_0^1 \frac{d\xi_1}{\xi_1} \int_1^\infty \frac{d\xi_2}{\xi_2} \left[\frac{dC}{d\varphi} \left(\frac{1}{1 + \hat{q}_t^2}, \xi_1, \xi_2, Q^2, \varphi \right) \delta \left(\hat{q}_t^2 - \xi_1 - \xi_2 - 2\sqrt{\xi_1 \xi_2} \cos \varphi \right) - \frac{dC}{d\varphi} \left(\frac{1}{1 + \hat{q}_t^2}, 0, \xi_2, Q^2 \right) \delta \left(\hat{q}_t^2 - \xi_2 \right) \right] \tag{B.16}$$

$$I_3 = \int_1^\infty \frac{d\xi_1}{\xi_1} \int_0^1 \frac{d\xi_2}{\xi_2} \left[\frac{dC}{d\varphi} \left(\frac{1}{1 + \hat{q}_t^2}, \xi_1, \xi_2, Q^2, \varphi \right) \delta \left(\hat{q}_t^2 - \xi_1 - \xi_2 - 2\sqrt{\xi_1 \xi_2} \cos \varphi \right) - \frac{dC}{d\varphi} \left(\frac{1}{1 + \hat{q}_t^2}, \xi_1, 0, Q^2 \right) \delta \left(\hat{q}_t^2 - \xi_1 \right) \right] \tag{B.17}$$

$$I_4 = \int_1^\infty \frac{d\xi_1}{\xi_1} \int_1^\infty \frac{d\xi_2}{\xi_2} \frac{dC}{d\varphi} \left(\frac{1}{1 + \hat{q}_t^2}, \xi_1, \xi_2, Q^2, \varphi \right) \delta \left(\hat{q}_t^2 - \xi_1 - \xi_2 - 2\sqrt{\xi_1 \xi_2} \cos \varphi \right). \tag{B.18}$$

The $\xi_1 \leftrightarrow \xi_2$ symmetry implies $I_2 = I_3$, and further allows us to write I_1

$$I_1 = 2 \int_0^1 \frac{d\xi_1}{\xi_1} \int_{\xi_1}^1 \frac{d\xi_2}{\xi_2} \left[\frac{dC}{d\varphi} \left(\frac{1}{1 + \hat{q}_t^2}, \xi_1, \xi_2, Q^2, \varphi \right) \times \delta \left(\hat{q}_t^2 - \xi_1 - \xi_2 - 2\sqrt{\xi_1 \xi_2} \cos \varphi \right) - \frac{dC}{d\varphi} \left(\frac{1}{1 + \hat{q}_t^2}, \xi_1, 0, Q^2 \right) \delta \left(\hat{q}_t^2 - \xi_1 \right) - \frac{dC}{d\varphi} \left(\frac{1}{1 + \hat{q}_t^2}, 0, \xi_2, Q^2 \right) \delta \left(\hat{q}_t^2 - \xi_2 \right) \right]. \tag{B.19}$$

as an integral over a triangle. In this way, only one subtraction is needed to make the integral finite; the other one is a finite integrable contribution.

As these integrals have to be further integrated in φ , one would be tempted to perform this integration first, before proceeding to $\xi_{1,2}$ integration. This seems advantageous because the “full” delta function can be easily solved for φ (this is what we have already done before) and the subtraction terms are φ -independent and thus the integral is trivial. However, proceeding in this way may potentially lead to numerical instabilities. Consider for instance I_2 , where the subtraction is needed to regulate the ξ_1 integral in $\xi_1 = 0$. After integrating analytically over φ , the remaining ξ_2 integration shall be done analytically (using the delta function) for the subtraction

term, but numerically (as we have already used the delta function) for the first term. The cancellation between the two terms is then realised after a numerical integration, which may be dangerous. To make the cancellation smoother, it is much safer to use the delta functions to fix the same variable (ξ_2) in the first term and in the subtraction term. The same holds for the I_1 integral, in the representation Eq. (B.19).

To do so, we need to solve the delta function for ξ_2 . The zeros of the argument are given by

$$\sqrt{\xi_2^\pm} = -\sqrt{\xi_1} \cos \varphi \pm \sqrt{\hat{q}_t^2 - \xi_1(1 - \cos^2 \varphi)}. \tag{B.20}$$

It is then convenient to change integration variable to $\sqrt{\xi_2}$. We get, for a generic function $F(\xi_2)$,

$$\int d\xi_2 F(\xi_2) \delta \left(\hat{q}_t^2 - \xi_1 - \xi_2 - 2\sqrt{\xi_1 \xi_2} \cos \varphi \right) = \frac{\theta \left(\hat{q}_t^2 - \xi_1(1 - \cos^2 \varphi) \right)}{\sqrt{\hat{q}_t^2 - \xi_1(1 - \cos^2 \varphi)}} \left[\sqrt{\xi_2^+} F(\xi_2^+) + \sqrt{\xi_2^-} F(\xi_2^-) \right] \tag{B.21}$$

where the denominator comes from the derivative of the argument of the delta function. According to this result we can find

$$\begin{aligned}
 I_1 = & 2 \int_0^1 \frac{d\xi_1}{\xi_1} \left[\frac{\theta(\hat{q}_t^2 - \xi_1(1 - \cos^2 \varphi))}{\sqrt{\hat{q}_t^2 - \xi_1(1 - \cos^2 \varphi)}} \left(\frac{1}{\sqrt{\xi_2^+}} \frac{dC}{d\varphi} \left(\frac{1}{1 + \hat{q}_t^2}, \xi_1, \xi_2^+, Q^2, \varphi \right) \right. \right. \\
 & \times \theta \left(1 - \sqrt{\xi_2^+} \right) \theta \left(\sqrt{\xi_2^+} - \sqrt{\xi_1} \right) + \frac{1}{\sqrt{\xi_2^-}} \frac{dC}{d\varphi} \left(\frac{1}{1 + \hat{q}_t^2}, \xi_1, \xi_2^-, Q^2, \varphi \right) \\
 & \times \theta \left(1 - \sqrt{\xi_2^-} \right) \theta \left(\sqrt{\xi_2^-} - \sqrt{\xi_1} \right) \left. \right) - \frac{1}{\hat{q}_t^2} \frac{dC}{d\varphi} \left(\frac{1}{1 + \hat{q}_t^2}, 0, \hat{q}_t^2, Q^2 \right) \\
 & \times \theta \left(1 - \hat{q}_t^2 \right) \theta \left(\hat{q}_t^2 - \xi_1 \right) \left. \right] + \frac{2}{\hat{q}_t^2} \frac{dC}{d\varphi} \left(\frac{1}{1 + \hat{q}_t^2}, \hat{q}_t^2, 0, Q^2 \right) \log \hat{q}_t^2 \theta \left(1 - \hat{q}_t^2 \right) \tag{B.22}
 \end{aligned}$$

$$\begin{aligned}
 I_2 = & \int_0^1 \frac{d\xi_1}{\xi_1} \left[\frac{\theta(\hat{q}_t^2 - \xi_1(1 - \cos^2 \varphi))}{\sqrt{\hat{q}_t^2 - \xi_1(1 - \cos^2 \varphi)}} \left(\frac{1}{\sqrt{\xi_2^+}} \frac{dC}{d\varphi} \left(\frac{1}{1 + \hat{q}_t^2}, \xi_1, \xi_2^+, Q^2, \varphi \right) \theta \left(\sqrt{\xi_2^+} - 1 \right) \right. \right. \\
 & \left. \left. + \frac{1}{\sqrt{\xi_2^-}} \frac{dC}{d\varphi} \left(\frac{1}{1 + \hat{q}_t^2}, \xi_1, \xi_2^-, Q^2, \varphi \right) \theta \left(\sqrt{\xi_2^-} - 1 \right) \right) - \frac{1}{\hat{q}_t^2} \frac{dC}{d\varphi} \left(\frac{1}{1 + \hat{q}_t^2}, 0, \hat{q}_t^2, Q^2 \right) \theta \left(\hat{q}_t^2 - 1 \right) \right]. \tag{B.23}
 \end{aligned}$$

It is easy to check that the explicit integrals in ξ_1 are finite as $\xi_1 \rightarrow 0$. Indeed in this limit $\sqrt{\xi_2^\pm} \rightarrow \pm\sqrt{\hat{q}_t^2}$, so the ξ_2^- contributions die due to the theta functions, and the ξ_2^+ contributions become identical to the subtraction terms, thus making the square bracket vanishing in the limit.

The last integral, I_4 , can be performed similarly to I_1 . However, because here there are no subtraction terms, it is possible to use the delta function for any variable, and in this case it may be convenient to do it for φ .

Note that I can be simplified as

$$\begin{aligned}
 I = & I_1 + 2I_2 + I_4 \\
 = & 2 \int_0^1 \frac{d\xi_1}{\xi_1} \left[\frac{\theta(\hat{q}_t^2 - \xi_1(1 - \cos^2 \varphi))}{\sqrt{\hat{q}_t^2 - \xi_1(1 - \cos^2 \varphi)}} \right. \\
 & \times \left(\frac{1}{\sqrt{\xi_2^+}} \frac{dC}{d\varphi} \left(\frac{1}{1 + \hat{q}_t^2}, \xi_1, \xi_2^+, Q^2, \varphi \right) \theta \left(\sqrt{\xi_2^+} - \sqrt{\xi_1} \right) \right. \\
 & \left. \left. + \frac{1}{\sqrt{\xi_2^-}} \frac{dC}{d\varphi} \left(\frac{1}{1 + \hat{q}_t^2}, \xi_1, \xi_2^-, Q^2, \varphi \right) \theta \left(\sqrt{\xi_2^-} - \sqrt{\xi_1} \right) \right) \right. \\
 & \left. - \frac{1}{\hat{q}_t^2} \frac{dC}{d\varphi} \left(\frac{1}{1 + \hat{q}_t^2}, 0, \hat{q}_t^2, Q^2 \right) \theta \left(\hat{q}_t^2 - \xi_1 \right) \right] \\
 & + \frac{2}{\hat{q}_t^2} \frac{dC}{d\varphi} \left(\frac{1}{1 + \hat{q}_t^2}, \hat{q}_t^2, 0, Q^2 \right) \log \hat{q}_t^2 \theta \left(1 - \hat{q}_t^2 \right) + I_4. \tag{B.24}
 \end{aligned}$$

Note also that the inequality $\sqrt{\xi_2^-} > \sqrt{\xi_1}$ required by the theta function in the second line implies

$$-\cos \varphi > 1 + \sqrt{\frac{\hat{q}_t^2}{\xi_1} - 1 + \cos^2 \varphi} \tag{B.25}$$

which is clearly impossible, so the result simplifies further

$$\begin{aligned}
 I = & 2 \int_0^1 \frac{d\xi_1}{\xi_1} \left[\frac{\theta(\hat{q}_t^2 - \xi_1(1 - \cos^2 \varphi))}{\sqrt{\hat{q}_t^2 - \xi_1(1 - \cos^2 \varphi)}} \frac{1}{\sqrt{\xi_2^+}} \right. \\
 & \times \frac{dC}{d\varphi} \left(\frac{1}{1 + \hat{q}_t^2}, \xi_1, \xi_2^+, Q^2, \varphi \right) \theta \left(\frac{\hat{q}_t^2}{2(1 + \cos \varphi)} - \xi_1 \right) \\
 & \left. - \frac{1}{\hat{q}_t^2} \frac{dC}{d\varphi} \left(\frac{1}{1 + \hat{q}_t^2}, 0, \hat{q}_t^2, Q^2 \right) \theta \left(\hat{q}_t^2 - \xi_1 \right) \right] \\
 & + \frac{2}{\hat{q}_t^2} \frac{dC}{d\varphi} \left(\frac{1}{1 + \hat{q}_t^2}, \hat{q}_t^2, 0, Q^2 \right) \log \hat{q}_t^2 \theta \left(1 - \hat{q}_t^2 \right) + I_4, \tag{B.26}
 \end{aligned}$$

where we have also traded the $\sqrt{\xi_2^+} > \sqrt{\xi_1}$ condition for a simpler condition on ξ_1 . The second theta function is more stringent than the first one, so the first one can be dropped. The result above can thus be written as

$$\begin{aligned}
 I = & 2 \int_0^{\frac{\hat{q}_t^2}{2(1 + \cos \varphi)}} \frac{d\xi_1}{\xi_1} \left[\frac{1}{\sqrt{\hat{q}_t^2 - \xi_1(1 - \cos^2 \varphi)}} \frac{1}{\sqrt{\xi_2^+}} \right. \\
 & \times \frac{dC}{d\varphi} \left(\frac{1}{1 + \hat{q}_t^2}, \xi_1, \xi_2^+, Q^2, \varphi \right) \\
 & \left. - \frac{1}{\hat{q}_t^2} \frac{dC}{d\varphi} \left(\frac{1}{1 + \hat{q}_t^2}, 0, \hat{q}_t^2, Q^2 \right) \right] \\
 & + \frac{2}{\hat{q}_t^2} \frac{dC}{d\varphi} \left(\frac{1}{1 + \hat{q}_t^2}, 0, \hat{q}_t^2, Q^2 \right) \log \frac{\hat{q}_t^2}{2(1 + \cos \varphi)} + I_4. \tag{B.27}
 \end{aligned}$$

The integral I_4 , having no subtraction in it, can be computed as in Eq. (B.9), using the delta function to fix φ .

Of course we can use the approach of using the delta function to integrate over ξ_2 also for the resummed result. In this case we find

$$\begin{aligned} \frac{Q^4 dC_{\text{reg}}}{dQ^2 dy dq_t^2} \left(x, Q^2, y, q_t^2, \alpha_s, \frac{Q^2}{\mu_F^2} \right) &= \frac{\theta \left(\frac{e^{-2|y|}}{x} - 1 - \hat{q}_t^2 \right)}{1 + \hat{q}_t^2} \int_{\xi_0}^{\infty} d\xi_1 \\ &\times \int_0^{2\pi} d\varphi \frac{\theta \left(\hat{q}_t^2 - \xi_1 (1 - \cos^2 \varphi) \right)}{\sqrt{\hat{q}_t^2 - \xi_1 (1 - \cos^2 \varphi)}} U'_{\text{reg}} \left(\sqrt{x(1 + \hat{q}_t^2)} e^y, Q^2 \xi_1, \mu_F^2 \right) \\ &\times \left[\sqrt{\xi_2^+} U'_{\text{reg}} \left(\sqrt{x(1 + \hat{q}_t^2)} e^{-y}, Q^2 \xi_2^+, \mu_F^2 \right) \frac{dC}{d\varphi} \left(\frac{1}{1 + \hat{q}_t^2}, \xi_1, \xi_2^+, Q^2, \varphi \right) \theta \left(\sqrt{\xi_2^+} - \sqrt{\xi_0} \right) \right. \\ &\left. + \sqrt{\xi_2^-} U'_{\text{reg}} \left(\sqrt{x(1 + \hat{q}_t^2)} e^{-y}, Q^2 \xi_2^-, \mu_F^2 \right) \frac{dC}{d\varphi} \left(\frac{1}{1 + \hat{q}_t^2}, \xi_1, \xi_2^-, Q^2, \varphi \right) \theta \left(\sqrt{\xi_2^-} - \sqrt{\xi_0} \right) \right] \end{aligned} \tag{B.28}$$

In fact, it is convenient to partition the integration region along the diagonal $\xi_1 = \xi_2$, to get

$$\begin{aligned} \frac{Q^4 dC_{\text{reg}}}{dQ^2 dy dq_t^2} \left(x, Q^2, y, q_t^2, \alpha_s, \frac{Q^2}{\mu_F^2} \right) &= \frac{\theta \left(\frac{e^{-2|y|}}{x} - 1 - \hat{q}_t^2 \right)}{1 + \hat{q}_t^2} \int_0^{2\pi} d\varphi \\ &\times \left[I_+ \left(x, Q^2, y, q_t^2, \alpha_s, \frac{Q^2}{\mu_F^2}, \varphi \right) + I_- \left(x, Q^2, y, q_t^2, \alpha_s, \frac{Q^2}{\mu_F^2}, \varphi \right) \right] \end{aligned} \tag{B.29}$$

$$\begin{aligned} I_+ \left(x, Q^2, y, q_t^2, \alpha_s, \frac{Q^2}{\mu_F^2}, \varphi \right) &= \int_{\xi_0}^{\frac{\hat{q}_t^2}{2(1+\cos\varphi)}} d\xi_1 \sqrt{\frac{\xi_2^+}{\hat{q}_t^2 - \xi_1 (1 - \cos^2 \varphi)}} \frac{dC}{d\varphi} \left(\frac{1}{1 + \hat{q}_t^2}, \xi_1, \xi_2^+, Q^2, \varphi \right) \\ &\times U'_{\text{reg}} \left(\sqrt{x(1 + \hat{q}_t^2)} e^y, Q^2 \xi_1, \mu_F^2 \right) \\ &\times U'_{\text{reg}} \left(\sqrt{x(1 + \hat{q}_t^2)} e^{-y}, Q^2 \xi_2^+, \mu_F^2 \right) \end{aligned} \tag{B.30}$$

$$I_- \left(x, Q^2, y, q_t^2, \alpha_s, \frac{Q^2}{\mu_F^2}, \varphi \right) = I_+ \left(x, Q^2, -y, q_t^2, \alpha_s, \frac{Q^2}{\mu_F^2}, -\varphi \right). \tag{B.31}$$

References

1. G. Salam, A Resummation of large subleading corrections at small x . JHEP **9807**, 019 (1998). <https://doi.org/10.1088/1126-6708/1998/07/019>. arXiv:hep-ph/9806482
2. M. Ciafaloni, D. Colferai, G. Salam, Renormalization group improved small x equation. Phys. Rev. D **60**, 114036 (1999). <https://doi.org/10.1103/PhysRevD.60.114036>. arXiv:hep-ph/9905566
3. M. Ciafaloni, D. Colferai, G.P. Salam, A.M. Stasto, The Gluon splitting function at moderately small x . Phys. Lett. B **587**, 87 (2004). <https://doi.org/10.1016/j.physletb.2004.02.054>. arXiv:hep-ph/0311325
4. M. Ciafaloni, D. Colferai, G. Salam, A. Stasto, Renormalization group improved small x Green's function. Phys. Rev. D **68**, 114003 (2003). <https://doi.org/10.1103/PhysRevD.68.114003>. arXiv:hep-ph/0307188
5. M. Ciafaloni, D. Colferai, G. Salam, A. Stasto, A Matrix formulation for small- x singlet evolution. JHEP **0708**, 046 (2007). <https://doi.org/10.1088/1126-6708/2007/08/046>. arXiv:0707.1453
6. R.D. Ball, S. Forte, Summation of leading logarithms at small x . Phys. Lett. B **351**, 313 (1995). [https://doi.org/10.1016/0370-2693\(95\)00395-2](https://doi.org/10.1016/0370-2693(95)00395-2). arXiv:hep-ph/9501231
7. R.D. Ball, S. Forte, Asymptotically free partons at high-energy. Phys. Lett. B **405**, 317 (1997). [https://doi.org/10.1016/S0370-2693\(97\)00625-4](https://doi.org/10.1016/S0370-2693(97)00625-4). arXiv:hep-ph/9703417
8. G. Altarelli, R.D. Ball, S. Forte, Factorization and resummation of small x scaling violations with running coupling. Nucl. Phys. B **621**, 359 (2002). [https://doi.org/10.1016/S0550-3213\(01\)00563-6](https://doi.org/10.1016/S0550-3213(01)00563-6). arXiv:hep-ph/0109178
9. G. Altarelli, R.D. Ball, S. Forte, An Anomalous dimension for small x evolution. Nucl. Phys. B **674**, 459 (2003). <https://doi.org/10.1016/j.nuclphysb.2003.09.040>. arXiv:hep-ph/0306156
10. G. Altarelli, R.D. Ball, S. Forte, Perturbatively stable resummed small x evolution kernels. Nucl. Phys. B **742**, 1 (2006). <https://doi.org/10.1016/j.nuclphysb.2006.01.046>. arXiv:hep-ph/0512237
11. G. Altarelli, R.D. Ball, S. Forte, Small x resummation with quarks: deep-inelastic scattering. Nucl. Phys. B **799**, 199 (2008). <https://doi.org/10.1016/j.nuclphysb.2008.03.003>. arXiv:0802.0032
12. R.S. Thorne, Explicit calculation of the running coupling BFKL anomalous dimension. Phys. Lett. B **474**, 372 (2000). [https://doi.org/10.1016/S0370-2693\(00\)00019-8](https://doi.org/10.1016/S0370-2693(00)00019-8). arXiv:hep-ph/9912284
13. R.S. Thorne, NLO BFKL equation, running coupling and renormalization. Phys. Rev. Scales **D60**, 054031 (1999). <https://doi.org/10.1103/PhysRevD.60.054031>. arXiv:hep-ph/9901331
14. R.S. Thorne, The running coupling BFKL anomalous dimensions and splitting functions. Phys. Rev. D **64**, 074005 (2001). <https://doi.org/10.1103/PhysRevD.64.074005>. arXiv:hep-ph/0103210
15. C.D. White, R.S. Thorne, A global fit to scattering data with NLL BFKL resummations. Phys. Rev. D **75**, 034005 (2007). <https://doi.org/10.1103/PhysRevD.75.034005>. arXiv:hep-ph/0611204
16. I.Z. Rothstein, I.W. Stewart, An effective field theory for forward scattering and factorization violation. arXiv:1601.04695
17. L.N. Lipatov, Reggeization of the vector meson and the vacuum singularity in nonabelian gauge theories. Sov. J. Nucl. Phys. **23**, 338 (1976)
18. V.S. Fadin, E. Kuraev, L. Lipatov, On the Pomeranchuk singularity in asymptotically free theories. Phys. Lett. B **60**, 50 (1975). [https://doi.org/10.1016/0370-2693\(75\)90524-9](https://doi.org/10.1016/0370-2693(75)90524-9)
19. E.A. Kuraev, L.N. Lipatov, V.S. Fadin, Multi-Reggeon processes in the Yang-Mills theory. Sov. Phys. JETP **44**, 443 (1976)
20. E.A. Kuraev, L.N. Lipatov, V.S. Fadin, The Pomeranchuk singularity in nonabelian gauge theories. Sov. Phys. JETP **45**, 199 (1977)
21. I.I. Balitsky, L.N. Lipatov, The Pomeranchuk singularity in quantum chromodynamics. Sov. J. Nucl. Phys. **28**, 822 (1978)
22. V.S. Fadin, L. Lipatov, BFKL pomeron in the next-to-leading approximation. Phys. Lett. B **429**, 127 (1998). [https://doi.org/10.1016/S0370-2693\(98\)00473-0](https://doi.org/10.1016/S0370-2693(98)00473-0). arXiv:hep-ph/9802290
23. R.D. Ball, V. Bertone, M. Bonvini, S. Marzani, J. Rojo, L. Rottoli, Parton distributions with small- x resummation: evidence for BFKL dynamics in HERA data. Eur. Phys. J. C **78**, 321 (2018). <https://doi.org/10.1140/epjc/s10052-018-5774-4>. arXiv:1710.05935
24. xFitter Developers' Team collaboration, H. Abdolmaleki et al., Impact of low- x resummation on QCD analysis of HERA data. Eur. Phys. J. C **78**, 621 (2018). <https://doi.org/10.1140/epjc/s10052-018-6090-8>. arXiv:1802.00064
25. M. Bonvini, F. Giuli, A new simple PDF parametrization: improved description of the HERA data. Eur. Phys. J. Plus **134**, 531 (2019). <https://doi.org/10.1140/epjp/i2019-12872-x>. arXiv:1902.11125
26. S. Catani, M. Ciafaloni, F. Hautmann, Gluon contributions to small- x heavy flavor production. Phys. Lett. B **242**, 97 (1990). [https://doi.org/10.1016/0370-2693\(90\)91601-7](https://doi.org/10.1016/0370-2693(90)91601-7)
27. S. Catani, M. Ciafaloni, F. Hautmann, High energy factorization and small- x heavy flavour production. Nucl. Phys. B **366**, 135 (1991)
28. S. Catani, F. Hautmann, High-energy factorization and small x deep inelastic scattering beyond leading order. Nucl. Phys. B **427**, 475 (1994). [https://doi.org/10.1016/0550-3213\(94\)90636-X](https://doi.org/10.1016/0550-3213(94)90636-X). arXiv:hep-ph/9405388
29. M. Bonvini, S. Marzani, T. Peraro, Small- x resummation from HELL. Eur. Phys. J. C **76**, 597 (2016). <https://doi.org/10.1140/epjc/s10052-016-4445-6>. arXiv:1607.02153
30. M. Bonvini, S. Marzani, C. Muselli, Towards parton distribution functions with small- x resummation: HELL 2.0. JHEP **12**, 117 (2017). [https://doi.org/10.1007/JHEP12\(2017\)117](https://doi.org/10.1007/JHEP12(2017)117). arXiv:1708.07510
31. M. Bonvini, Small- x phenomenology at the LHC and beyond: HELL 3.0 and the case of the Higgs cross section. Eur. Phys. J. C **78**, 834 (2018). <https://doi.org/10.1140/epjc/s10052-018-6315-x>. arXiv:1805.08785
32. F. Caola, S. Forte, S. Marzani, Small x resummation of rapidity distributions: the case of Higgs production. Nucl. Phys. B **846**, 167 (2011). <https://doi.org/10.1016/j.nuclphysb.2011.01.001>. arXiv:1010.2743
33. S. Forte, C. Muselli, High energy resummation of transverse momentum distributions: Higgs in gluon fusion. JHEP **03**, 122 (2016). [https://doi.org/10.1007/JHEP03\(2016\)122](https://doi.org/10.1007/JHEP03(2016)122). arXiv:1511.05561
34. C. Muselli, Double differential high energy resummation. arXiv:1710.09376
35. J.C. Collins, R.K. Ellis, Heavy quark production in very high energy hadron collisions. Nucl. Phys. B **360**, 3 (1991)
36. S. Catani, M. Ciafaloni, F. Hautmann, High-energy factorization in QCD and minimal subtraction scheme. Phys. Lett. B **307**, 147 (1993). [https://doi.org/10.1016/0370-2693\(93\)90204-U](https://doi.org/10.1016/0370-2693(93)90204-U)
37. S. Catani, F. Hautmann, Quark anomalous dimensions at small x . Phys. Lett. B **315**, 157 (1993). [https://doi.org/10.1016/0370-2693\(93\)90174-G](https://doi.org/10.1016/0370-2693(93)90174-G)
38. R.D. Ball, Resummation of hadroproduction cross-sections at high energy. Nucl. Phys. B **796**, 137 (2008). <https://doi.org/10.1016/j.nuclphysb.2007.12.014>. arXiv:0708.1277
39. M. Bonvini, R. Gauld, T. Giani, S. Marzani, Drell-Yan at small x (**In preparation**)
40. M. Ciafaloni, D. Colferai, Dimensional regularisation and factorisation schemes in the BFKL equation at subleading level. JHEP **09**, 069 (2005). <https://doi.org/10.1088/1126-6708/2005/09/069>. arXiv:hep-ph/0507106
41. S. Marzani, R.D. Ball, P. Falgari, S. Forte, BFKL at next-to-next-to-leading order. Nucl. Phys. B **783**, 143 (2007). <https://doi.org/10.1016/j.nuclphysb.2007.05.024>. arXiv:0704.2404

42. M. Deak, F. Hautmann, H. Jung, K. Kutak, Forward jet production at the large hadron collider. *JHEP* **09**, 121 (2009). <https://doi.org/10.1088/1126-6708/2009/09/121>. arXiv:0908.0538
43. M. Deak, F. Hautmann, H. Jung, K. Kutak, Forward jets and energy flow in hadronic collisions. *Eur. Phys. J. C* **72**, 1982 (2012). <https://doi.org/10.1140/epjc/s10052-012-1982-5>. arXiv:1112.6354
44. F.G. Celiberto, D.Y. Ivanov, M.M.A. Mohammed, A. Papa, High-energy resummed distributions for the inclusive Higgs-plus-jet production at the LHC. *Eur. Phys. J. C* **81**, 293 (2021). <https://doi.org/10.1140/epjc/s10052-021-09063-2>. arXiv:2008.00501
45. F.G. Celiberto, High-energy emissions of light mesons plus heavy flavor at the LHC and the forward physics facility. *Phys. Rev. D* **105**, 114008 (2022). <https://doi.org/10.1103/PhysRevD.105.114008>. arXiv:2204.06497
46. F.G. Celiberto, M. Fucilla, Diffractive semi-hard production of a J/ψ or a Υ from single-parton fragmentation plus a jet in hybrid factorization. *Eur. Phys. J. C* **82**, 929 (2022). <https://doi.org/10.1140/epjc/s10052-022-10818-8>. arXiv:2202.12227
47. A. van Hameren, L. Motyka, G. Ziarko, Hybrid k_T -factorization and impact factors at NLO. *JHEP* **11**, 103 (2022). [https://doi.org/10.1007/JHEP11\(2022\)103](https://doi.org/10.1007/JHEP11(2022)103). arXiv:2205.09585
48. M. Bonvini, S. Marzani, Four-loop splitting functions at small x . *JHEP* **06**, 145 (2018). [https://doi.org/10.1007/JHEP06\(2018\)145](https://doi.org/10.1007/JHEP06(2018)145). arXiv:1805.06460
49. P. Nason, S. Dawson, R.K. Ellis, The total cross-section for the production of heavy quarks in hadronic collisions. *Nucl. Phys. B* **303**, 607 (1988). [https://doi.org/10.1016/0550-3213\(88\)90422-1](https://doi.org/10.1016/0550-3213(88)90422-1)
50. S. Frixione, P. Nason, G. Ridolfi, A positive-weight next-to-leading-order Monte Carlo for heavy flavour hadroproduction. *JHEP* **09**, 126 (2007). <https://doi.org/10.1088/1126-6708/2007/09/126>. arXiv:0707.3088
51. S. Catani, S. Devoto, M. Grazzini, S. Kallweit, J. Mazzitelli, Bottom-quark production at hadron colliders: fully differential predictions in NNLO QCD. *JHEP* **03**, 029 (2021). [https://doi.org/10.1007/JHEP03\(2021\)029](https://doi.org/10.1007/JHEP03(2021)029). arXiv:2010.11906
52. R. Ball, R.K. Ellis, Heavy quark production at high-energy. *JHEP* **0105**, 053 (2001). <https://doi.org/10.1088/1126-6708/2001/05/053>. arXiv:hep-ph/0101199
53. S.P. Baranov, Highlights from the k_T factorization approach on the quarkonium production puzzles. *Phys. Rev. D* **66**, 114003 (2002). <https://doi.org/10.1103/PhysRevD.66.114003>
54. B.A. Kniehl, D.V. Vasin, V.A. Saleev, Charmonium production at high energy in the k_T -factorization approach. *Phys. Rev. D* **73**, 074022 (2006). <https://doi.org/10.1103/PhysRevD.73.074022>. arXiv:hep-ph/0602179
55. A.D. Bolognino, F.G. Celiberto, M. Fucilla, D.Y. Ivanov, A. Papa, High-energy resummation in heavy-quark pair hadroproduction. *Eur. Phys. J. C* **79**, 939 (2019). <https://doi.org/10.1140/epjc/s10052-019-7392-1>. arXiv:1909.03068
56. P. Nason, A new method for combining NLO QCD with shower Monte Carlo algorithms. *JHEP* **11**, 040 (2004). <https://doi.org/10.1088/1126-6708/2004/11/040>. arXiv:hep-ph/0409146
57. S. Frixione, P. Nason, C. Oleari, Matching NLO QCD computations with Parton Shower simulations: the POWHEG method. *JHEP* **11**, 070 (2007). <https://doi.org/10.1088/1126-6708/2007/11/070>. arXiv:0709.2092
58. S. Alioli, P. Nason, C. Oleari, E. Re, A general framework for implementing NLO calculations in shower Monte Carlo programs: the POWHEG BOX. *JHEP* **06**, 043 (2010). [https://doi.org/10.1007/JHEP06\(2010\)043](https://doi.org/10.1007/JHEP06(2010)043). arXiv:1002.2581
59. PROSA collaboration, O. Zenaiev et al., Impact of heavy-flavour production cross sections measured by the LHCb experiment on parton distribution functions at low x . *Eur. Phys. J. C* **75**, 396 (2015). <https://doi.org/10.1140/epjc/s10052-015-3618-z>. arXiv:1503.04581
60. R. Gauld, J. Rojo, L. Rottoli, J. Talbert, Charm production in the forward region: constraints on the small- x gluon and backgrounds for neutrino astronomy. *JHEP* **11**, 009 (2015). [https://doi.org/10.1007/JHEP11\(2015\)009](https://doi.org/10.1007/JHEP11(2015)009). arXiv:1506.08025
61. R. Gauld, J. Rojo, Precision determination of the small- x gluon from charm production at LHCb. *Phys. Rev. Lett.* **118**, 072001 (2017). <https://doi.org/10.1103/PhysRevLett.118.072001>. arXiv:1610.09373
62. Particle Data Group collaboration, R.L. Workman et al., Review of particle physics. *PTEP* **2022**, 083C01 (2022). <https://doi.org/10.1093/ptep/ptac097>